

RAMAN MICROSPECTROSCOPY IN THE ANALYSIS OF PLANT CUTICULAR MEMBRANES

by

Kadek Okuda Andersen

B.Sc. (Honours), McGill University

A THESIS SUBMITTED IN PARTIAL FULFILLMENT OF THE REQUIREMENTS FOR
THE DEGREE OF

MASTER OF SCIENCE

in

THE FACULTY OF GRADUATE STUDIES

(Chemistry)

THE UNIVERSITY OF BRITISH COLUMBIA

(Vancouver)

April 2010

© Kadek Okuda Andersen 2010

ABSTRACT

The outside of plants, including fruit, are covered by a cuticular membrane (CM). This membrane serves as protection from environmental factors. The basic composition of the CM is well understood, however, there are always variations among different species. The CM consists of a cutin matrix, which is the structural component, and cuticular waxes. The study of the CM for both structural and compositional features has been accomplished for a variety of species. The instrumentation methods used to complete these analyses have been mostly destructive and at most been able to provide spatial distribution information along the vertical axis. Raman microspectroscopy has been used previously to quantify and map triterpenoid concentrations in *Prunus laurocerasus* leaf CMs. This data showed transverse variations in concentration across the CM. The goal of the current work is to explore the viability of using Raman microspectroscopy to analyze other species and classes of compounds.

Initially, alkylresorcinols in rye leaf waxes, artificial wax mixtures, and rye leaf CMs were examined. Using the current instrumentation it was not possible to quantify and detect alkylresorcinols in rye CMs, but it may become a viable option in the future. Based on the previous work with triterpenoids, this class of compounds was attempted next. Triterpenoids in tomato CMs were investigated resulting in the discovery that, while triterpenoids are not detectable in the tomato CM due to the presence of polysaccharides, lycopene can be detected. It was found that it is present in the remains of the epidermal cells after digestion of the cell walls (epidermal remnants), but not in the CM itself. The analysis of other species for triterpenoids was attempted including the leaves of *Rosa canina*, *Ligustum vulgare*, *Kalanchoe daigremontiana*, and the fruit of the *Prunus avium* and *Prunus laurocerasus*. While quantification of triterpenoids was not successful, a lot was learned about the variables which go into a successful Raman analysis of triterpenoids in plant CMs. These variables include the relative amount of triterpenoids to wax and wax to CM, along with the wax coverage ($\mu\text{g}/\text{cm}^2$). These results will aid in future attempts at Raman analysis of triterpenoids in CMs.

TABLE OF CONTENTS

Abstract.....	ii
Table of Contents.....	iii
List of Tables	v
List of Figures.....	vi
List of Abbreviations	viii
Acknowledgements.....	ix
Dedication.....	x
Chapter 1: Introduction.....	1
1.1 Raman Spectroscopy.....	1
1.2 Raman Microspectroscopy.....	4
1.3 Confocal Raman Spectroscopy	4
1.4 The Structure of the Plant Cuticle.....	6
1.5 Alkylresorcinols, Lycopene, and Triterpenoids.....	8
1.6 Previous Work.....	10
Chapter 2: Alkylresorcinols in Rye Leaves.....	14
2.1 Introduction.....	14
2.2 Materials and Methods.....	16
2.2.1 Raman microscope.....	16
2.2.2 Confocal setup	17
2.2.3 Software.....	18
2.2.4 Raman spectroscopy system parameters	18
2.2.5 Reference materials	18
2.2.6 Artificial wax mixtures.....	19
2.2.7 Wax extraction.....	19
2.2.8 Digestion of cell walls	20
2.3 Results and Discussion.....	20
2.4 Conclusion	28
Chapter 3: Lycopene and Triterpenoids in Tomatoes	29
3.1 Introduction.....	29

3.2	Materials and Methods.....	31
3.2.1	Raman spectroscopy system parameters	31
3.2.2	Reference materials	31
3.2.3	Wax extraction.....	31
3.2.4	Digestion of cell walls	32
3.3	Results and Discussion.....	32
3.4	Conclusion	39
Chapter 4: Application of Raman Microspectroscopy to the Analysis of Triterpenoids in Cuticular Membranes.....		40
4.1	Introduction.....	40
4.2	Materials and Methods.....	41
4.2.1	Raman spectroscopy system parameters	41
4.2.2	Reference materials	41
4.2.3	Plant and fruit samples.....	41
4.2.4	Digestion of cell walls	42
4.2.5	Wax extraction, and GC analysis.....	42
4.3	Results.....	43
4.3.1	Cherry fruit (<i>Prunus avium</i>)	43
4.3.2	<i>Kalanchoe daigremontiana</i>	46
4.3.3	<i>Ligustrum vulgare</i> and <i>Rosa canina</i> leaves	48
4.3.4	<i>Prunus laurocerasus</i> fruit.....	50
4.4	Discussion	51
4.5	Conclusion	54
Chapter 5: Conclusions and Future Work		56
5.1	Concluding Remarks.....	56
5.2	Future Work	58
References.....		60

LIST OF TABLES

Table 2.1	The composition of rye wax and the nujol mull (artificial rye wax).....	25
Table 4.1	The approximate percentages of triterpenoids within the wax, wax within the CM, and wax coverage in some analyzed specie.....	53

LIST OF FIGURES

Figure 1.1	Jablonski energy level diagram depicting Raman scattering.....	2
Figure 1.2	Illustration of confocal Raman concept.....	5
Figure 1.3	Illustration showing the pavement cells along with the cuticle and wax regions.....	7
Figure 1.4	Illustration of digestion of plant cell walls leaving the cuticular membrane.....	8
Figure 1.5	General chemical structure of alkylresorcinols.....	9
Figure 1.6	Chemical structure of lycopene.....	10
Figure 2.1	Bright field image of rye leaf cuticular membrane.....	15
Figure 2.2	Optical path of the Raman microscope.....	17
Figure 2.3	Illustration of rye plant showing leaf segment used for analysis.....	20
Figure 2.4	Raman spectra of alkylresorcinols of different chain lengths and resorcinol.....	21
Figure 2.5	Raman spectra of varying chain length alkanes.....	23
Figure 2.6	Raman spectra of alkylresorcinols and hexacosanol.....	24
Figure 2.7	Raman spectra of extracted rye wax and the nujol mull (artificial rye wax) along with their difference.....	26
Figure 2.8	Raman spectra of rye CM.....	27
Figure 3.1	Structure of triterpenoids α -, β -, and δ -amyrin.....	30
Figure 3.2	Normalized Raman spectra of mature green, yellow, and red tomato fruit CMs.....	33
Figure 3.3	Normalized Raman spectra of α - and β -amyrin along with red tomato fruit CM.....	34
Figure 3.4	Normalized Raman spectra of tomato fruit wax, red tomato fruit CM, and hentriacontane.....	35
Figure 3.5	Raman spectra of red tomato fruit CM, cutin matrix, and their difference.....	36

Figure 3.6	Normalized Raman spectra of difference (tomato fruit CM – CM without wax) and lycopene.....	37
Figure 3.7	Normalized Raman spectra of tomato fruit CM epidermal remnants (remnants of cells after digestion of cell walls) and lycopene.....	38
Figure 4.1	Raman spectra of cherry fruit wax, nonacosane, and ursolic acid.....	44
Figure 4.2	Structures of nonacosane and ursolic acid.....	44
Figure 4.3	Raman spectra of cherry fruit CM, cutin matrix and the difference between the two along with the spectrum of cherry fruit wax.....	45
Figure 4.4	Raman spectra of ursolic acid and nonacosane, along with the difference spectrum from Figure 4.3.....	46
Figure 4.5	Structures of glutinol and friedelin.....	47
Figure 4.6	Raman spectra of glutinol, <i>Kalanchoe</i> leaf CM, and hentriacontane.....	47
Figure 4.7	Raman spectra of <i>Ligustrum vulgare</i> leaf and its cutin matrix.....	49
Figure 4.8	Raman spectra of <i>Rosa canina</i> (rose) leaf CM, hentriacontane, and the rose cutin matrix.....	50
Figure 4.9	Raman spectra of ursolic acid and <i>Prunus laurocerasus</i> fruit CM.....	51

LIST OF ABBREVIATIONS

AFM	Atomic Force Microscopy
CCD	Charge-Coupled Device
CM	Cuticular Membrane
GC	Gas Chromatography
HPLC	High Performance Liquid Chromatography
IR	Infrared
MS	Mass Spectrometry
NA	Numerical Aperture
NIR	Near Infrared
NMR	Nuclear Magnetic Resonance
SEM	Scanning Electron Microscopy
SNR	Signal-to-Noise Ratio
TEM	Transmission Electron Microscopy
UV-Vis	Ultraviolet-Visible
VLC	Very Long Chain

ACKNOWLEDGEMENTS

I would like to thank my supervisors Dr. Mike Blades and Dr. Robin Turner for their guidance and for making this work possible. As well as Dr. Reinhard Jetter who provided all of the insights into the plant world.

Thanks to the entire Turner group for the help and support. I would like to especially thank Dr. Georg Schulze, Dr. Stanislav Konorov and Dr. Marcia Yu who assisted me with a variety of aspects of this project and were always there to answer my questions. I would also like to extend my gratitude to the members of the Jetter lab who have assisted me along way with analysis and plant related quandaries, especially Christopher Buschhaus, Xiufeng Ji, and Miao Wen. Finally I would like to thank my family and friends for all of their love and support.

This thesis is dedicated to my parents Kiyō and Annie Okuda,
without whom I would not be the person I am today.

Chapter 1: Introduction

The use of Raman microspectroscopy for the examination and quantification of compounds in plants including fruit is an emerging field of study. Raman microspectroscopic analysis of cuticular membranes of *Prunus laurocerasus* leaves has been previously accomplished, but the general applicability of this technique has not yet been fully explored.¹ The importance of studying the exterior of plants is derived from the need to understand the function of different compounds within these surfaces. The plant cuticle shows physical features of the cells which lie below it. The distribution of compounds across this cuticle can provide insight into the function of those compounds in relation to the visible structural features. Background theory and information needed to understand this work will be provided in this chapter.

1.1 Raman Spectroscopy

The Raman effect was discovered in 1928 by C.V. Raman and his colleague K.S. Krishnan.² It was observed that when light was focused on a sample the resulting scattered radiation had two main components, namely the Rayleigh (elastic) scattering having the same wavelength as the incident light and the Raman (inelastic) scattering having an altered wavelength.² It was found that an intense illumination source was required to observe the significantly smaller fraction of photons that are inelastically scattered (~ 1 in 10^8).³ Consequently an increase in the interest in Raman scattering followed the invention of stronger excitation sources, particularly with the invention of the laser in 1962.^{4,5}

The Raman Effect is caused by a polarizability change in the scattering molecule. The mechanism by which Raman scattering takes place can be described using either the classical view or the quantum mechanical view. Classical theory is based on the induction of a dipole in the molecule of interest when it is struck by the incident radiation (usually a laser). The induced dipole ($\mu(t)$) is approximated by Equation 1 (the derivation of which can be found in reference ⁴).

$$\mu(t) = \alpha_o E_o \cos 2\pi\nu_o t + \frac{1}{2} \left(\frac{\partial \alpha}{\partial q} \right) q_o E_o [\cos\{2\pi(\nu_o + \nu_m)t\} + \cos\{2\pi(\nu_o - \nu_m)t\}] \quad (1)$$

Where α_o is the polarizability, E_o is the vibrational amplitude of the excitation source (laser), ν_o is the frequency of the laser, t is time, q_o is the vibrational amplitude of the displacement between the nuclei of a molecule, and ν_m is the frequency of the molecular vibration.⁴ Equation 1 can be broken down into three terms. The first term ($\alpha_o E_o \cos 2\pi\nu_o t$) represents Rayleigh scattering occurring with the same frequency (ν_o) as the incident radiation. The other two terms correspond to Raman scattering, the first of which has a higher frequency ($\nu_o + \nu_m$) than the incident radiation and is known as anti-Stokes Raman scattering. The final term has a lower frequency ($\nu_o - \nu_m$) when compared with the incident radiation and is known as Stokes Raman scattering. To further understand this concept another explanation of the Raman effect using a Jablonski energy level diagram, Figure 1.1, is provided below.

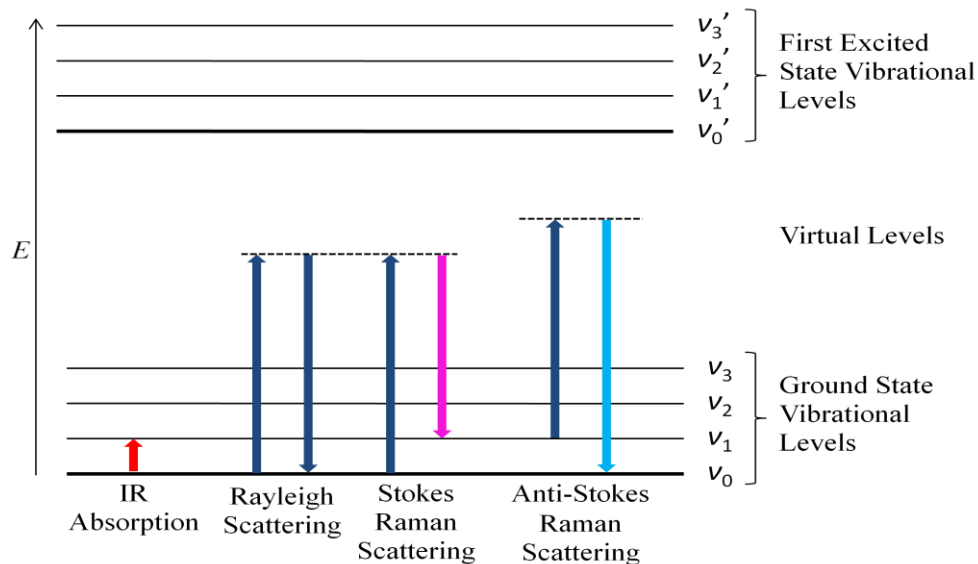


Figure 1.1 The energy level diagram depicting Raman scattering. The red arrow shows Infrared (IR) absorption. The upward pointing dark blue arrows represent excitation. The downward pointing dark blue arrow shows Rayleigh scattering, while the pink and light blue arrows show Stokes and anti-Stokes Raman scattering, respectively.

The relationship between excitation and scattered light can be visualized using Figure 1.1, where Rayleigh scattering, Stokes Raman, and anti-Stokes Raman scattering are depicted. As mentioned previously, it can be seen that Rayleigh scattering (shown as the dark

blue arrow) has the same wavelength (energy) as the incident radiation (dark blue arrow). In the quantized energy level view the anti-Stokes Raman scattering originates from the first excited vibrational level (ν_1). This level is less populated than the ground vibrational level (Maxwell-Boltzmann distribution law), making the spectral lines arising from anti-Stokes scattering weaker than those arising from Stokes scattering. The anti-Stokes lines also correspond to a higher frequency Raman scattering as seen by the light blue arrow being longer than the pink arrow. The vertical axis in Figure 1.1 is energy so longer arrows correspond to higher energies (E) which correspond to higher frequencies ($E=h\nu$, where h is Planck's constant). The Stokes lines are those more commonly used for analysis due to their larger intensity.

Figure 1.1 also depicts Infrared (IR) absorption (shown as a red arrow). IR absorption and Raman spectroscopy both probe vibrational transitions but, because the quantum mechanical selection rules originate from different sources, they are commonly seen as complementary techniques. Raman scattering results from a polarizability change in the molecule whereas IR absorption results from a change in the dipole moment of a molecule. The different selection rules result in molecules being IR- or Raman-active or both IR- and Raman-active, so the techniques are not, in general, mutually exclusive. The main advantage of both IR absorption and Raman spectroscopy is that chemical information can be obtained without destruction of the sample. This is assuming that the sample does not photodegrade. Consequently, samples must be checked for photodegradation. However, one major advantage of Raman spectroscopy over IR spectroscopy is the lack of a large water signal; consequently Raman spectroscopy can be applied easily to aqueous samples unlike IR spectroscopy.

The vibrational information gained by Raman spectroscopy can be used in a variety of ways. The Raman signals can be used as a fingerprint to identify molecules. The intensity of the signals can also be used to give quantitative information, which will be discussed further later.

1.2 Raman Microspectroscopy

The coupling of Raman spectroscopy with microscopy has greatly improved the applicability of the Raman technique. The first Raman microscope was built and used by Thomas Hirschfeld in 1973, although the concept had been developed earlier in 1966.⁶ The main advantage of Raman microspectroscopy over conventional Raman is the increase in spatial resolution obtained by focusing the laser through an objective lens. Lasers can be focussed to a diffraction limited spot size, allowing for the analysis of very small samples or for examining small domains in a macroscopic sample.^{3,7} The Raman scattered light can be collected through the same objective lens as used for focusing the excitation. Thus, the area analyzed when using a Raman microscope, the spot size, is well defined. The examination of adjacent spots on a sample allows a Raman microscope to give spatial information, which can be used to create maps of a given Raman signal over a defined area. Mapping experiments can be carried out in numerous ways. These procedures are described in detail elsewhere.¹ Mapping experiments can be used to show the concentration variation of a compound over a specified area. The theory and application of these types of experiments will not be discussed here as this was not exploited in the work presented in this thesis. All work done in this thesis was completed using a Raman microscope which will be described later in the materials and methods section of Chapter 2.

The main advantage of conventional Raman microscopy is the increased lateral spatial resolution of the technique compared to conventional Raman spectroscopy. However, this increase in resolution along the focal plane is not accompanied by increased resolution along the optical axis (vertical). Resolution along the optical axis can be gained through the use of a confocal imaging microscope which is discussed in the next section.

1.3 Confocal Raman Spectroscopy

Marvin Minsky invented the first confocal microscope in 1957.⁸ The defining feature of the confocal microscope is that any signal originating from a plane other than the focal plane of the microscope will not be detected. The original confocal microscope used a pinhole placed before the detector (back image plane of the microscope) to block light from

planes outside of the focal plane.^{8,9} The system used for my research uses a slit coupled with a Charged-Coupled Device (CCD) camera to produce the same effect. The slit width and the CCD image area are adjustable to allow flexibility in the confocal modality. The general concept is depicted below in Figure 1.2.

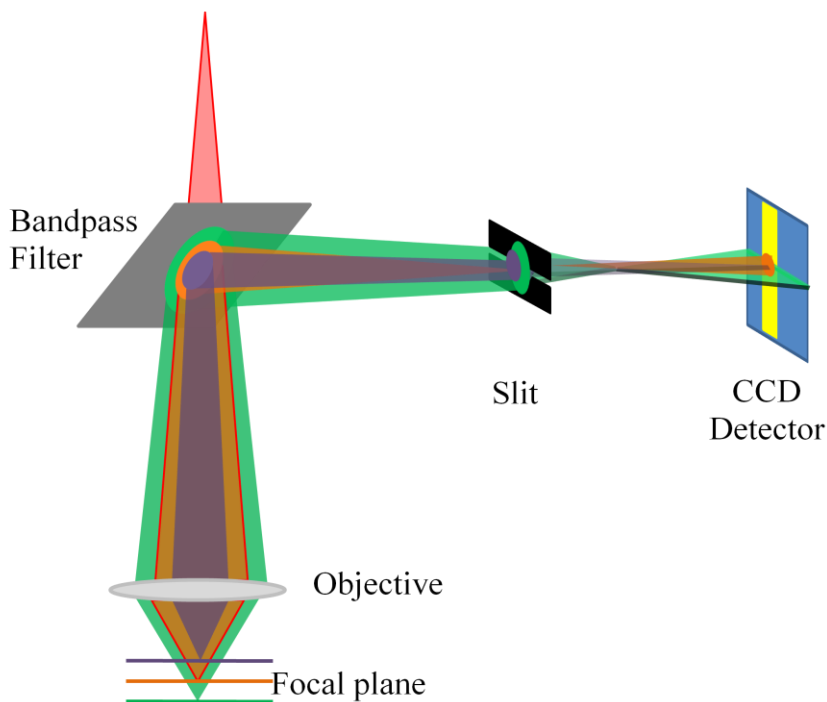


Figure 1.2 Illustration of confocal Raman concept. The red shows the incident light, while the orange trace shows the light hitting the focal plane. The purple and green traces show light hitting above and below the focal plane. The yellow strip on the CCD detector shows the area selected to detect the signal.

Figure 1.2 shows the incident radiation coming in from above (in red). Following the path of the backscattered light from the focal plane (shown in orange), it can be seen that the scattered radiation focuses on the slit allowing all the radiation from this plane to pass through the slit. The radiation is then focused on the selected area of the CCD (shown as a yellow strip). The vertical purple and green scattered radiation gets blocked by the slit leaving a horizontal strip approaching the detector. This strip of scattered radiation is then cut again when it reaches the CCD detector such that very little of the scattered radiation from the out of focus planes is actually detected. This way the entire signal from the focal plane is gathered while most of the signals from out of focus planes are removed. Logically,

when using confocal microscopy, there is a decrease in signal strength from the background as well as the molecule of interest, as signal is lost from the locations outside the focal plane. However, when it comes to analyzing vertical gradients or thin samples it is a very useful tool.

While confocal Raman microscopy is useful, it is not possible to realize the ideal operation described above. The technique collects scattered radiation from more than simply the focal plane. This is because the laser does not focus to a point, due to diffraction effects it focuses to a small volume element, commonly called the beam waist.⁹ The beam waist is defined by the properties of the laser and the objective, especially the numerical aperture (NA).^{9,10} The diameter of this waist directly affects the resolving power of the microscope and attempts have been made to correct for the waist mathematically.¹⁰ Most measurements in this thesis were made without the confocal mode of the microscope and no attempts were made to correct for the waist resolution as it was unnecessary for the current application. However, even with these limitations, when the microscope was setup in confocal mode an x-y resolution of approximately 3 by 5 microns could be achieved (based on measurements with a silicon wafer). The penetration depth (z-resolution) depends on the sample characteristics, but should be on the order of tens of microns or less.

1.4 The Structure of the Plant Cuticle

The surfaces of plants, including fruits, are covered with a protective extra-cellular membrane known as a cuticle. The cuticle or cuticular membrane (CM) serves as protection from environmental factors. It has many functions including control over water loss and the exchange of gases, as well as defence against pathogens and excessive UV light.^{11,12} The ability of the cuticle to carry out all of these functions makes it very important for survival. Consequently the composition of the cuticle is an area of great interest.

The cuticle is believed to be synthesized by the epidermal cells of a plant which are exposed to air.¹³ The epidermal cells can be classified into different types consisting mainly of guard cells and pavement cells (refer to Figure 1.4). The pavement cells make up most of the epidermal cells while the guard cells form stomata (pores in the leaf) allowing for the

entrance of carbon dioxide for photosynthesis and the exit of oxygen produced.¹⁴ A third type of cells known as trichomes are present in only some species. Trichomes are epidermal cells that protrude from the surface, resulting in a hair-like structure. All of the epidermal cells discussed have a rigid outer cell wall which provides structural support. There are two regions of the outer cell wall, the periclinal and anticlinal. The periclinal region is the area of the cell wall which is on the exposed surface of the cells while the anticlinal region lies between adjacent cells as is shown in Figure 1.3. On the outer (environmentally exposed) surface of these epidermal cells sits the cuticle. The compositions of cuticles vary by species and age, although the same basic building blocks are found in all cases. The cuticle is composed of cutin (a polymer matrix insoluble in organic solvents) and wax. The wax is found within the cutin matrix (intracuticular wax) and on top of it (epicuticular wax). The different regions are depicted in Figure 1.3.

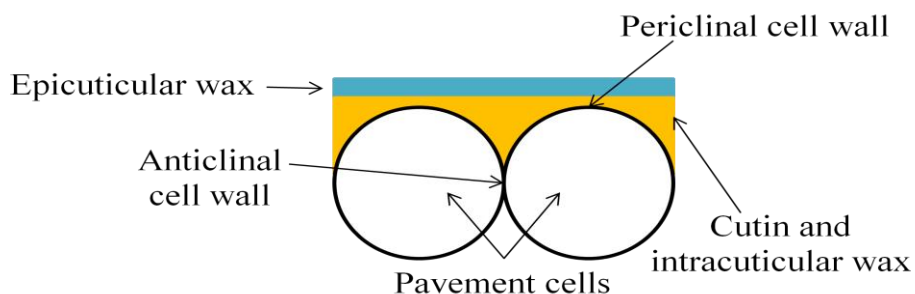


Figure 1.3 An illustration showing periclinal and anticlinal cell walls along with intracuticular and epicuticular regions. The cuticle is the orange and blue sections together.

The wax found in the cuticle is for the most part composed of very long chain (VLC) aliphatic compounds of varying lengths (alkanes, primary alcohols, aldehydes, fatty acids, esters, etc.).¹⁵ While these are the main constituents of the waxes, there are also secondary alcohols and ketones with more rare compounds including triterpenoids and alkylresorcinols. It is these more rare components of the wax that are the focus of this work.

Cutin, which accounts for most of the CM's mass, is primarily composed of hydroxylated fatty acids (C_{16} , C_{18}) linked by ester bonds making up the polymer matrix.¹⁶⁻¹⁸ It was discovered that another type of insoluble polymer known as cutan, composed mostly of polymeric aliphatic constituents, is also present in some cuticles.^{18,19} The polymeric matrix which holds the wax in place is not of great interest to the current work as it generally has the

same composition across most species. Consequently it will not be further discussed. The waxes as mentioned are either embedded within or on top of the cutin matrix. The CM itself is initially attached to the outer epidermal cell wall through a layer of pectin. Later in the development it is attached by a combination of cellulose and pectin.^{13,20} This is the result of the CM attaching to the more cellulose-rich region of the cell wall.^{13,20} Consequently a combination of cellulase and pectinase enzymes can be used to release the cuticular membranes for study.^{13,16} The CM lies on top of the epidermal cells and because it contains the cutin polymer is thus able to hold its shape. Consequently, when the CM is enzymatically removed, it still shows the cell imprints as depicted in Figure 1.4.

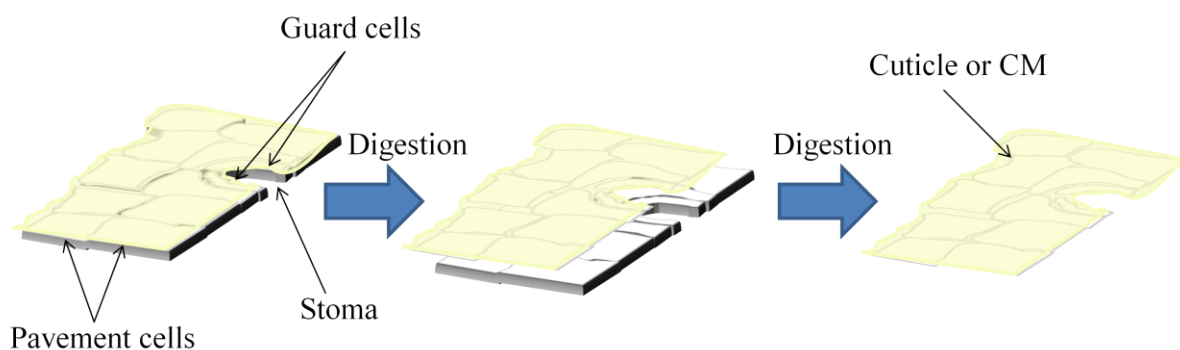


Figure 1.4 Illustration of digestion of plant epidermal cell walls leaving the CM.

Consequently, when looking at a CM's composition it is possible to show the concentrations of compounds relative to where the cells were once situated.²¹ Furthermore, this makes enzymatic removal of the CM a good sample preparation method for Raman microspectroscopy as it provides useful information about a cuticle without having to worry about background Raman signals from cells.

1.5 Alkylresorcinols, Lycopene, and Triterpenoids

The compounds studied in this work include alkylresorcinols, lycopene, and triterpenoids. These compounds are all found in plant leaves and fruit, and since their functions are not related they will be discussed separately.

Alkylresorcinols are a class of compounds found in mango flesh, the bran of cereal grains, cashew shells, and the wax of rye leaves among other plant tissues.²²⁻²⁷ Within this class of compounds it is the 5-n-alkylresorcinols that are of primary interest. Their general structure is shown in Figure 1.5.

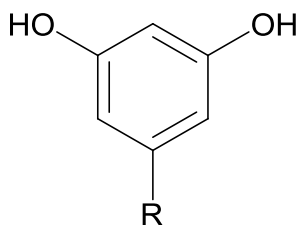


Figure 1.5 General structure of alkylresorcinols. Where **R** is an odd numbered saturated alkyl chain. When **R=H** the molecule is called resorcinol.

They consist of 1,3-dihydroxybenzene with a saturated odd-numbered alkyl chain of varying length in the 5 position. Alkylresorcinols are believed to cause contact dermatitis, have antibacterial and antifungal properties, show antioxidant activity, and are potentially useful as a marker for whole grain intake.^{26,28-31} Previous analyses of alkylresorcinols have been carried out by gas chromatography (GC), HPLC, and fluorescence spectroscopy.^{22,24,26,27} The occurrence of alkylresorcinols in cuticular wax has been reported in barley seeds as well as rye leaves.^{27,29} Consequently, initial Raman analysis was carried out on rye leaves as will be discussed in Chapter 2.

Triterpenoids are derived from six isoprene units arranged and substituted in various configurations and are of interest due to their positive health effects. Specifically, oleanolic acid and ursolic acid have been shown to have hepatoprotective, anti-inflammatory, antitumor, and anti-microbial effects.³²⁻³⁵ Similarly, α - and β -amyrin have been shown to suppress pruritus.³⁶ Lupeol is also known to have hepatoprotective effects.³⁷ Triterpenoids are found in many species, and have been found in many plants already used for medicinal purposes.³⁸⁻⁴⁰ Consequently, triterpenoid concentrations in plants and food stuffs are of interest. Their detection in the CMs of tomatoes and other species is discussed in Chapters 3 and 4.

Lycopene is the main carotenoid responsible for the red color of tomatoes. It is also an antioxidant which acts by scavenging radicals and quenching singlet oxygen.⁴¹⁻⁴³ The structure of lycopene is shown in Figure 1.6.

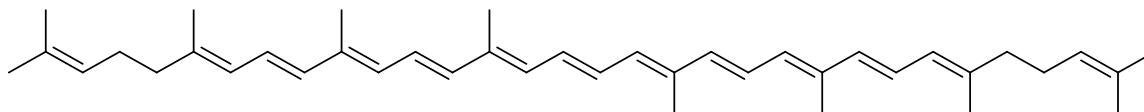


Figure 1.6 Structure of lycopene.

The lycopene concentration in an animal's body is related entirely to dietary intake, as it is only synthesized in plants, algae, fungi, and photosynthetic bacteria. Lycopene also has potential anti-carcinogenic effects and, therefore, the concentration and location of lycopene in foods is of great interest.^{44,45} Previous investigations into lycopene have used Raman, IR, NIR (Near Infrared), and UV-Vis (Ultraviolet-Visible) spectroscopy as well as HPLC.⁴⁶⁻⁵¹ The analysis of lycopene in tomato samples using Raman microspectroscopy is discussed in Chapter 3.

1.6 Previous Work

The analysis of plant, including fruit, surfaces has been done using a multitude of different techniques. Each technique has its own advantages and disadvantages and provides a specific type of information. This work focuses specifically on cuticles and their analysis. Consequently, techniques previously used to analyse the cuticle will be briefly discussed. The analysis of cuticles can be broken down into methods which analyze the two main components of the cuticle (cutin matrix and wax). The structural part of the cuticle can be analysed visually using different microscopic methodologies. These include visible light microscopy, scanning electron microscopy (SEM), atomic force microscopy (AFM), and transmission electron microscopy (TEM).^{20,52} These techniques provide images of the cuticle's surface resulting in structural and morphological information, but they do not provide chemical information. Visualizing the cuticle in these ways can only provide so much information and consequently other techniques have been applied.

As described above, the cuticle can be broken down into two major parts, the wax and the cutin matrix which holds the wax. This division can also be thought of as those parts of the cuticle which are soluble in organic solvents (waxes) and those which are insoluble (cutin matrix). It is important to note this difference as most studies which do not involve structural determination look at either one component or the other, but not both at the same time. The analysis of waxes is much simpler due to their solubility in organic solvents, while the analysis of the cuticular matrix (composed mostly of cutin) is more complex. The insolubility of cutin requires depolymerisation to break it down into oligomeric units before examination. Analysis of cutin oligomers has been reported using GC-MS, NMR (nuclear magnetic resonance), and HPLC techniques.^{19,53-55} These techniques have provided information on the cutin subunit composition. There are fewer techniques which can analyze the intact polymer although this has been accomplished using solid state NMR.^{53,56} The results of these analyses have provided a comprehensive understanding of the cuticular matrix and its composition. In all of these cases, the cutin must be separated from all surrounding components (cells, waxes, etc.).

The analysis of waxes has also been accomplished by a multitude of different methods on a variety of species. The techniques employed can be divided into those which study the composition of waxes, including GC-MS and HPLC, and those which look at the wax morphology, such as SEM, NMR, and X-ray diffraction.⁵⁷⁻⁶⁰ The composition of wax varies across species and even within a species depending on its growth stage. Consequently any specimen of interest must be analyzed individually to determine its exact wax composition. The wax components can affect such things as water permeability and wax morphology.^{60,61} The analysis of waxes is mostly done by extracting the waxes using organic solvents. This results in a mixture of intracuticular and epicuticular wax. The development of new methods to selectively extract one layer at a time has resulted in the discovery that there can be compositional differences between wax layers.^{27,62} The techniques mentioned so far provide chemical or structural information for cuticle components, but few can provide them *in situ*. This is especially true of wax analysis as most involve solvent extraction. One technique which can provide chemical information *in situ* is Raman spectroscopy.

Raman spectroscopy and microspectroscopy have been used in a variety of applications on plants, fruits, and vegetables.^{21,46,63-67} The analysis of compounds using Raman spectroscopy ideally involves a signal in the spectrum which originates only from the compound of interest without any interference from background or other signals. The mapping of the intensity of this signal over the surface of an object shows the amount of the compound relative to the amount in its surrounding area. The difficulty is that this signal intensity reflects the absolute amount within the volume of interrogation (i.e. in grams) without direct reference to sample thickness. When examining samples with a thickness greater than the laser penetration depth this technique will provide, as mentioned, intensity maps of the amounts of a compound, however it will not relay information on the transverse gradient of that compound. Alternatively, when the sample is thinner than the laser penetration depth, any inhomogeneity in the sample thickness is not accounted for. Consequently, Raman spectroscopy cannot differentiate between regions where the compound of interest is more concentrated or where the sample is thicker which results in a larger signal without an increase in concentration. Methods have been developed to try and overcome this obstacle. As an example, if the sample has a constant and homogeneously distributed concentration of a specific component, then all spectra can be normalized to this signal such that any change in thickness is accounted for by the variation in this signal. This method results in relative concentrations (i.e. ratio or %) as opposed to absolute concentrations (i.e. $\mu\text{g}/\text{cm}^2$).

Absolute concentrations have been measured in plant samples by the use of chemometric methods and the analysis of many samples by HPLC as well as Raman to obtain calibration curves.^{46,68} While this analysis has provided quantitative information, it requires the analysis of many samples by two methods and not just by Raman spectroscopy. However, once an accurate calibration curve has been created, further analysis of samples requires only the use of Raman spectroscopy. In the case of carotenoids (lycopene and β -carotene), absolute quantification using Raman spectroscopy was less accurate than IR analysis.⁴⁶ An additional quantification method involves using spectra from all of the components that make up the sample. Consequently, the composition of the sample has to be known and standards of these compounds must be available. The relative quantification of components has been achieved in this way for the CMs of *Prunus laurocerasus* leaves.^{1,21}

Each technique has its own limitations, but the analysis using only Raman spectroscopy is the one employed for this work and consequently will be discussed further.

Work was completed in this area by Dr. Marcia Yu at The University of British Columbia.¹ The relative quantification and concentration mapping of triterpenoids in the CM of *Prunus laurocerasus* leaves was completed. The quantitative results showed agreement with previously published literature data, while the mapping data showed the distribution of triterpenoids in relation to epidermal cells.²¹ This technique has thus far only been applied to *Prunus laurocerasus* leaves and consequently the versatility of this technique has not been established. The aim of this thesis is to apply Raman microspectroscopy in order to determine if this technique is amenable to other species and classes of compounds.

The work presented in this thesis has been separated into five chapters. This chapter has provided introductory and background information. Chapter 2 will discuss the application of Raman microspectroscopy to detection of alkylresorcinols in the CM of rye leaves. The lack of a consistently detectable signal for alkylresorcinols resulted in the examination of triterpenoids in tomato fruit CMs discussed in Chapter 3. The application of Raman microspectroscopy for triterpenoid detection to a CM samples from various other species, discussed in Chapter 4, provided a number of guidelines which could prove very useful for any future work in this area. Finally, Chapter 5 presents conclusions and potential areas for future work.

Chapter 2: Alkylresorcinols in Rye Leaves

The analysis of any new analyte requires preliminary work to ascertain if a given technique is feasible for a desired analysis. In this chapter, the probing of alkylresorcinols in the leaves of the rye plant using Raman microspectroscopy is discussed. To determine if this technique has the ability to show lateral alkylresorcinol concentration gradients on rye leaves, increasingly complex model samples were analysed and the results are discussed in this chapter.

2.1 Introduction

Alkylresorcinols, as discussed in Chapter 1, are compounds of increasing interest. The ability to detect them *in situ* could provide important information about their function in the plant cuticle. The application of Raman microspectroscopy for quantification in plant cuticles has been accomplished previously, but is not a well established technique.¹ Further development of the technique for this application requires that the general composition of cuticular waxes be known so that signals in the Raman spectrum can be assigned. The signal assignments, whether based on literature or experimental data, provide the potential for quantitative information to be obtained.

When beginning a new analysis, it is important to determine what kind of information can be gained and how a new technique can improve or add to current knowledge. It has been shown that rye grains have significantly higher concentrations of alkylresorcinols than other cereal grains.^{24,69} Previous work has demonstrated the presence of alkylresorcinols in rye leaf waxes.²⁷ The leaf waxes, as mentioned earlier, are part of the plant cuticular membrane (CM). The main goal of this work is to carry out investigations on plants, ideally *in situ*, thus the advantages and disadvantages of analyzing leaves or grains must be considered.

The logical progression for development of a Raman-based analysis appropriate for investigating the leaf requires the examination of increasingly complex samples culminating

with *in situ* measurements. The sequence begins with the analysis of solid standards, followed by waxes, CMs, and finally the intact leaves. First, solid standards are readily available for purchase from a variety of companies. Second, leaf wax has been shown to be easily extracted using organic solvents. Thirdly, the isolation of CMs is a well documented process with a relatively simple procedure. The CMs can be isolated by removing the underlying plant cells which could interfere with the Raman analysis. This can be easily accomplished by digesting the cell walls, a process that leaves the CM intact thus showing the structures and positions where the adjacent cells were as shown in Figure 2.1. Finally, use of intact leaves can be as simple as requiring only the correct age and segment of the plant leaf without any further preparation.



Figure 2.1 Bright field image of a rye leaf cuticular membrane. The lighter lines outline where the cells used to sit.

The isolation of the exterior of cereal grains on the other hand is not such a simple process and cannot provide the same information about the underlying cells. Given the previous work on alkylresorcinol concentrations in rye leaf wax and the well established analyses, rye leaves are a more appropriate candidate for Raman microscopic analysis than rye grains.

The alkylresorcinols found in rye leaves consist of 1,3-dihydroxybenzenes substituted with a saturated alkyl chain ranging from C₁₉-C₂₇ (odd numbers only) at the 5 position (refer to Figure 1.5). They constitute 3%, by weight, of the total rye leaf cuticular wax.²⁷ The wax analysis previously carried out on rye leaves involved removing the wax in layers, thus providing information on both the intracuticular and epicuticular wax composition. It was determined that alkylresorcinols were concentrated in the intracuticular wax.²⁷ Hence there is a vertical gradient of alkylresorcinols which raises the question: Is there a lateral

heterogeneity of alkylresorcinols as well? Raman microspectroscopy has been used previously to determine the lateral arrangements of triterpenoids in *Prunus laurocerasus* leaves; its application to alkylresorcinols in rye leaves is explored in this chapter.¹

2.2 Materials and Methods

2.2.1 Raman microscope

A Ramanscope System 1000 (Renishaw plc, Gloucestershire, UK) was used for most Raman measurements. During the course of this research, the system was upgraded to the inVia Renishaw Raman Microscope and the upgraded microscope was used only where indicated. The Renishaw system is linked to a Leica DMLB microscope (Leica Microsystems, Ontario, Canada). The microscope has 5x (0.12 NA), 20x (0.40 NA), and 50x (0.75 NA) objectives which were used for analysis. The system is equipped with a Renishaw 785 nm diode laser (RL785) whose power was checked each time the system was initiated using a Coherent Fieldmaster power meter. The laser power was also checked at the microscope objective using a hand held LaserCheck power meter. The power from the 50x objective varied from 35-45 mW. To allow for mapping experiments the microscope was equipped with a motorized xyz stage (ProScan Series, Prior Scientific Inc.). The stage could be programmed and controlled either by Renishaw software or manually by joystick. In addition to viewing the image through the microscope eyepiece, the system also had a video camera whose output could be seen on the computer monitor. The camera allowed for image capturing as well as the setting up of mapping experiments and sample positioning. The system was calibrated before each use using a silicon wafer. If the representative signal at 520 cm^{-1} was not in the correct location an offset was applied before any measurements were taken. The optical path of the spectrometer is shown in Figure 2.2.

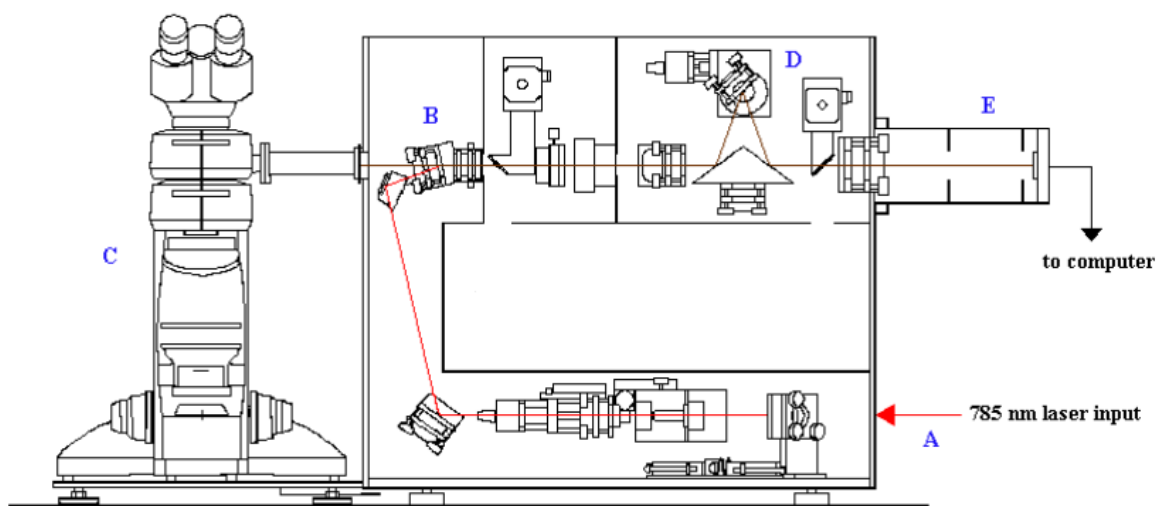


Figure 2.2 Optical path of the Raman microscope. The red and brown lines show the laser path and the Raman scattered light. A is where the laser enters, B is the holographic notch filter, C is the microscope, D is the grating and E is the CCD detector. Reproduced with permission of Renishaw plc.

The laser (shown in red) enters through the back of the instrument at A and is directed using mirrors to the holographic notch filters B and into the microscope C. The light is then directed through the microscope objective and focused onto the sample. The scattered light (shown as a brown line) is collected by the same objective lens and directed back through the microscope and again to B where the 785nm source light is filtered out and only the Raman scattered wavelengths pass through. The light continues to the grating D where it is dispersed and finally detected with the CCD detector at E.

2.2.2 Confocal setup

The microscope has an adjustable slit width as well as an adjustable image area on the CCD. The combination of these parameters can be used to setup the microscope to perform confocal acquisition as discussed earlier in Chapter 1. Confocal mode of the microscope was achieved using a 10 μm slit width, a 3 x 576 pixel image area on the CCD, and the 50x objective. Although this is supposed to provide a vertical spatial resolution of approximately 5 μm , the actual resolution depends on many different parameters such as the sample roughness and laser penetration depth.^{1,70} Vertical resolution measurements using

silicon wafer showed a worse resolution than the quoted value. However, this value varies by sample and consequently a specific figure of merit characterizing the instrument cannot be determined. Using the confocal mode of the microscope greatly reduces the signal from out of focus planes and hence lowers the signal-to-noise ratio (SNR). Hence, the measurements made for this thesis were mostly performed with the microscope not in confocal mode since z-axis resolution was not the main consideration and SNR was important. The confocal mode was, however, at least attempted for most measurements; the results were rarely used but are discussed where relevant.

2.2.3 Software

The Renishaw WiRETM (version 1.3.30 and 3.1 (after upgrade)) software and Grams/32[®] (Graphic Relational Array Management System, version 4.14, level II) were used to capture and view Raman signals detected by the CCD and the video camera images. Baseline correction and other data analysis were performed using Matlab release 13 (Mathworks, Natick, MA). The program implemented in Matlab used for background subtraction was written by Dr. Georg Schulze.⁷¹ All other programs used for analysis were also implemented in Matlab script.

2.2.4 Raman spectroscopy system parameters

All spectra were acquired in static mode centered on 1100 cm⁻¹. The laser power was set to 50% and all spectra were acquired with a 50x (0.75NA) objective. The image area on the CCD was set to have a three pixel width, thus increasing the resolution in the x-y plane and the binning was set to two. The integration time was set between 10-120 seconds (60 s for all samples, except resorcinol (10 s) and rye wax (120 s), and 2-100 accumulations were acquired (2 for all samples except rye wax (4), rye CM (100), and the alkanes (4)). The slit width was set to 50 μm for all samples except the rye CM where the slit was set to 100 μm.

2.2.5 Reference materials

Nonadecylresorcinol (1,3-dihydroxy-5-nonadecylbenzene) and pentacosylresorcinol standards were purchased from Resealife (Burgdorf, Switzerland). Tridecylresorcinol (Ji X.) and octacosanal (Wen M., pyridinium chlorochromate oxidation of octacosanol) were

synthesized in the Jetter lab at The University of British Columbia.²⁷ Docosyl docosanoate was purchased from Roth (Karlsruhe, Germany). Hexacosanol, nonacosane, hentriacontane, and hexacosanoic acid were obtained from Sigma-Aldrich (Oakville, Ontario, Canada). Resorcinol was obtained from BDH (Toronto, Canada). Raman spectra of each sample were obtained as a reference. All compounds were used as received. The spectra were collected (using parameters specified previously) at different points on the same solid sample and compared to ensure that there were no significant differences in the spectra of the same standard.

2.2.6 Artificial wax mixtures

Alkylresorcinols along with aliphatic compounds were weighed out on a microbalance (Sartorius MC5) and placed into a quartz mortar bowl. The resulting mixture had relative weight ratios similar to those found in the rye wax. The contents of the mortar bowl were then ground with a pestle into a fine powder and a minute amount of mineral oil (Aldrich) was mixed in creating a nujol mull. The nujol mull was mixed for a few minutes to obtain as homogenous a mixture as possible which was then transferred onto a microscope slide using a rubber policeman. Once on the slide, the mixture was concentrated into a small area and smoothed to yield a roughly uniform sample thickness.

2.2.7 Wax extraction

Rye seeds were bought from Capers (Vancouver) and germinated in soil. Plants were grown under ambient conditions in the Jetter lab at The University of British Columbia. The second leaves were harvested from plants, approximately three weeks after planting. To be consistent with previous work ~5 cm segments of the second rye leaf ~10 cm away from the stem of the plant were used as show in Figure 2.3.²⁷

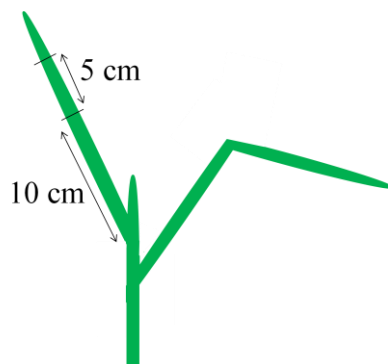


Figure 2.3 Illustration of rye plant showing leaf segment used for analysis.

Each segment was dipped for ~30 s in a beaker containing approximately 30 mL of chloroform (Fisher Scientific, Ottawa, Ontario, Canada) to initiate wax extraction. The segment was then transferred to a second beaker and the process was repeated to ensure all wax had been extracted. The chloroform extracts were then combined into one beaker and left in a fume hood to evaporate.

2.2.8 Digestion of cell walls

Rye cuticular membranes (CMs) were isolated using Orgell's technique as modified by Yamada et al. and Petracek and Bukovac.⁷²⁻⁷⁴ Rye leaf segments of 1-2 cm in length were cut from a ~5 cm segment of the second rye leaf ~10 cm away from the stem of the plant as described above. These pieces were then placed in a 20 mL scintillation vial containing 2% (w/w) cellulase (INC Biomedicals, Aurora, Ohio), 2% (w/w) pectinase (Fluka, Switzerland), and 1 mM sodium azide (NaN_3) in 5 mL citrate buffer. The leaf segments were transferred into a new enzyme solution every 3 days and digested for a total of 6 days. After digestion was complete, the isolated CMs were placed in NanopureTM water in a Petri dish and floated over a hole pierced into a piece of aluminum foil and left to dry.

2.3 Results and Discussion

The feasibility of examining the distribution of the compounds across a cuticle requires that there be distinguishable Raman signals that can be used to differentiate between the background and the compound of interest. Therefore initial analysis is performed on

synthetic standards, to determine the viability of further analysis. It is also important to ensure that the sample does not photodegrade. To check for photodegradation, all samples were run multiple times in the same spot. The resulting spectra were then overlaid to check for photodegradation. If photodegradation occurred, the Raman signals would shift or change intensity. In any cases of photodegradation the microscope settings were optimized to eliminate it. This was accomplished by either decreasing the laser power or the duration of time the laser spot spent on the sample. If these initial investigations indicated that further experimentation was viable, *in situ* measurements using waxes, cuticular membranes, and finally leaves would be performed. The specific application of this technique to rye leaves begins with taking the spontaneous Raman spectra of available n-alkylresorcinol standards along with resorcinol (1,3-dihydroxybenzene), and the results are shown below (Figure 2.4).

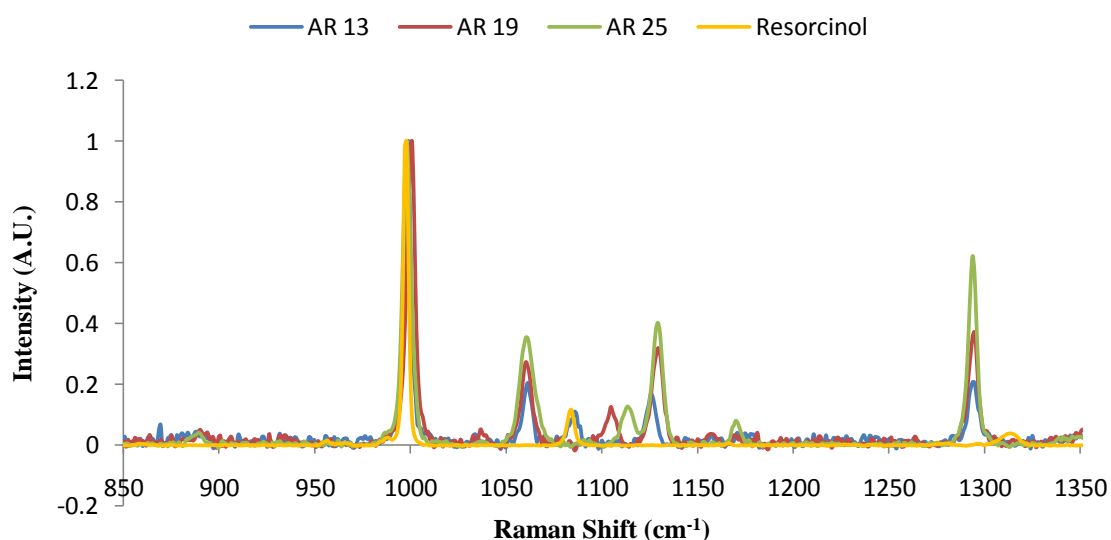


Figure 2.4 Raman spectra of alkylresorcinols of different chain lengths and resorcinol. Spectra were normalized to the tallest signal. AR = alkylresorcinol and # = alkyl chain length (i.e. 19 = C₁₉H₃₉).

It should be noted that in the above spectra (Figure 2.4) alkylresorcinols with different chain lengths share many of the same signals. There are four strong signals which overlap in all of the spectra pertaining to alkylresorcinols (1000 cm⁻¹, 1060 cm⁻¹, 1129 cm⁻¹, and 1293 cm⁻¹). There is also one signal (approximately 1110 cm⁻¹) which shifts to lower wavenumbers as the alkyl chain length decreases. This signal could thus potentially be used to distinguish

between alkylresorcinols with differing chain lengths in the same sample; however, to do this an understanding of the molecular origins of this signal is required. The band assignments for alkylresorcinols in the region of interest have not been reported in the literature, although assignments for resorcinol were found. The signal at 1085 cm^{-1} in the resorcinol spectrum originates from C-H bending in the aromatic ring.⁷⁵ The signal at 1000 cm^{-1} in the resorcinol spectrum, which overlaps with the alkylresorcinols spectra, can be attributed to the breathing mode of the aromatic ring.⁷⁵ There are three signals which appear in the alkylresorcinol spectra, which are not present in the resorcinol spectrum; these can be attributed to motions of the alkyl chain. The signals at 1060 cm^{-1} and 1129 cm^{-1} are believed to be derived from C-C stretching of the alkyl chain, and the signal at 1293 cm^{-1} is due to twisting of the $-(\text{CH}_2)_n-$ in the alkyl chain backbone.^{76,77} It should be noted that, as expected, many of the alkyl-specific signals show a trend of increasing intensity with chain length. The shifting of the signal at approximately 1110 cm^{-1} could originate from either the aromatic ring or the alkyl chain. In the first case, the lengthening of the alkyl chain could cause the aromatic C-H bending signal to shift from 1085 cm^{-1} in the resorcinol spectrum. This is less likely to be the case, because elongation of the chain affecting this signal so greatly is questionable because of the distance from the ring at which the change occurs. If the signal originates from the alkyl chain, in theory a similar trend should be observed for differing chain length alkanes. The Raman spectra of alkanes of different chain lengths were run and the results are shown below in Figure 2.5.

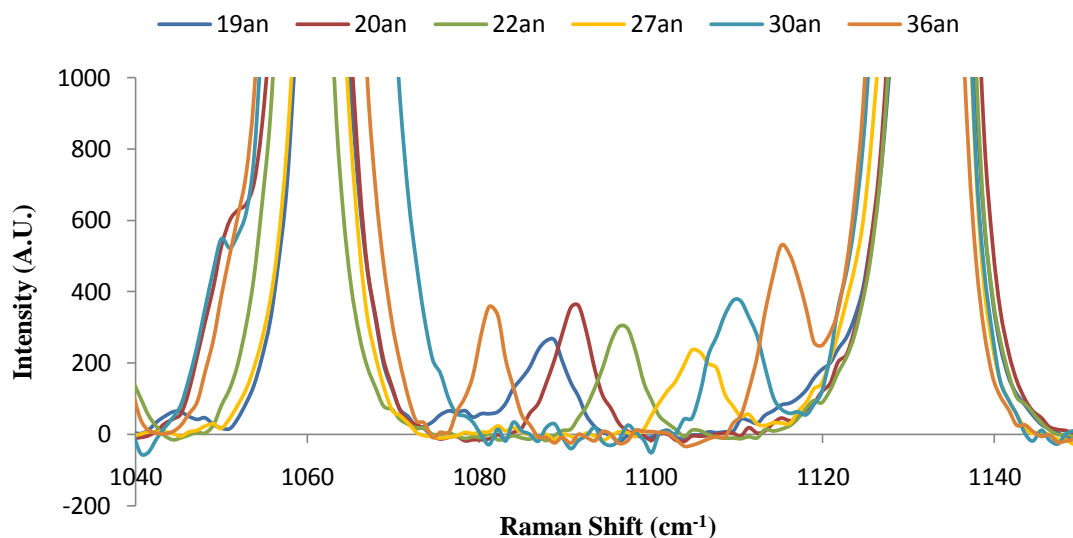


Figure 2.5 Raman spectra of varying chain length alkanes. The #an stands for the number of carbons in the hydrocarbon chain i.e. 19an = nonadecane (C₁₉H₄₀).

The same trend noted in the alkylresorcinol spectra can be seen above; the signals shift to lower wavenumbers as the chain length decreases. While the same trend is observed, the signals do not appear in the same position. For example the signal for nonadecane (19an) appears at 1090 cm⁻¹, while for 5-nonadecylresorcinol (AR 19) the signal appears at 1105 cm⁻¹. The signal at 1090 cm⁻¹ in the nonadecane Infrared spectrum has previously been assigned to C-C stretching.⁷⁸ In other sets of alkane derivatives a signal around 1100 was assigned to CH₂ twisting along the alkyl chain.^{79,80} Specifically for octadecanethiol a signal was observed at 1104 cm⁻¹ which showed the same trend, shifting to lower wavenumbers as the alkyl chain length was shortened. The experimental and literature data support the idea that this signal originates from the alkyl chain, as mentioned earlier, and could be used as a marker to distinguish between alkylresorcinols with different chain lengths. However, theoretical analysis would be required to pinpoint the exact reason for this shift.

Rye wax is composed mostly of very long chain (VLC) primary alcohols, alkyl esters, and aldehydes.²⁷ In addition to these main constituents, alkylresorcinols account for approximately 3% of the total wax by weight.²⁷ Within these VLC aliphatics there are some chain lengths that occur in larger concentration than others. Dominating compounds vary by species and class of compound. The Raman spectra of VLC aliphatic compounds are all very

similar, differing mostly in signal amplitude, not signal frequencies. The Raman spectra for a variety of aliphatic compounds was obtained, but because of the spectral similarities mentioned above, only the most abundant component of the rye wax, hexacosanol which makes up 69% by weight, is initially discussed.²⁷ The Raman spectrum of hexacosanol is shown in Figure 2.6 along with the alkylresorcinol spectra for comparison.

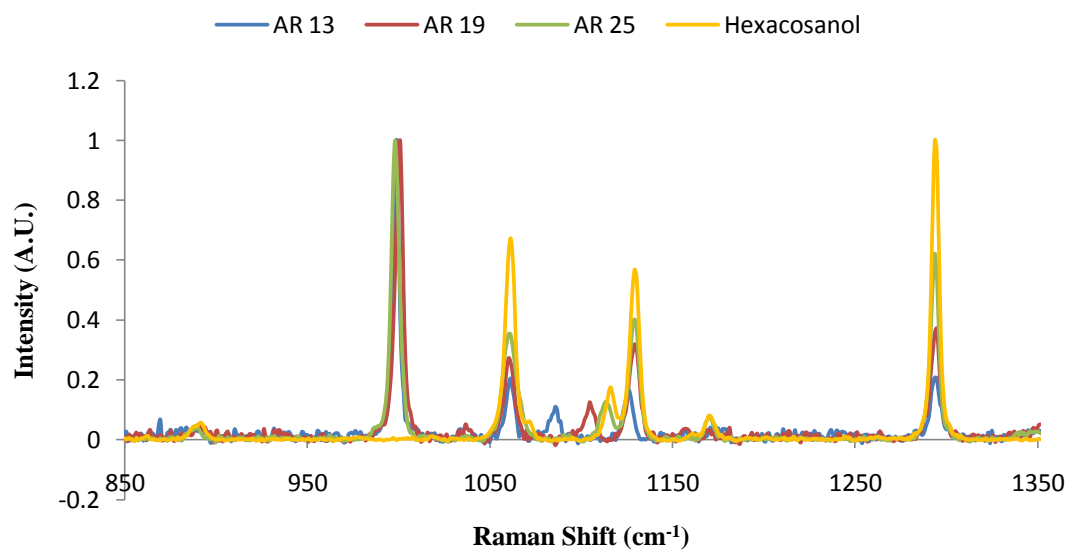


Figure 2.6 Raman spectra of alkylresorcinols and hexacosanol. Spectra were normalized to the tallest signal. AR = alkylresorcinol and # = alkyl chain length (i.e. 19 = C₁₉H₃₉).

Hexacosanol has three intense signals which overlap with the alkylresorcinol spectra because the signals originate from the alkyl chain as discussed earlier. There is another intense signal at approximately 1000 cm⁻¹ which appears only in the alkylresorcinol spectra and not in that of hexacosanol. It should be noted that reanalysis of some wax aliphatic compounds using the updated inVia microscope (described in section 2.2) showed an additional signal at 995 cm⁻¹ (data not shown), however, this signal should not interfere with the currently discussed analysis and is reported here for completeness, but will not be discussed further. The 1000 cm⁻¹ signal as discussed earlier is derived from the aromatic ring. Since alkylresorcinols are the only compounds with aromatic structures known to be present in rye wax this signal should serve as a marker for these compounds. This marker signal suggests that Raman analysis is possible for alkylresorcinols in rye. The next step is to determine its feasibility using mixed standards, rye wax, and rye CMs.

The relative quantities of each component in the rye wax have been previously reported in the literature.²⁷ This knowledge was used to make an artificial rye wax mixture which contained relative amounts of each component similar to those reported. Theoretically, the Raman spectrum generated from this mixture should be identical to the Raman spectrum of rye wax. Furthermore, varying the amounts of specific components in this mixture would allow for a model system which could be used to transform Raman data into quantitative data. To this end, solid standards were chosen which best represented each of the compound classes in the rye wax. In cases where the standard for the most abundant compound was not available, the best available standard was used. These solid standards were used to form a nujol mull for analysis as described in the materials and methods (Section 2.2). Table 2.1 shows the relative amounts of each compound class found in rye wax, compounds which were used as standards to represent each class (including their relative amounts in rye wax), and experimental data for the nujol mull.

Table 2.1 The composition of rye wax and the nujol mull (artificial rye wax).

The first and second columns show the compound classes present in rye wax and their relative amounts. The third and fourth columns show the standard used to represent that compound class and the actual percentage of the representative standard present in rye wax. The final column shows the experimental data for the nujol mull. The values in column two and four were obtained from Ji X.F. and Jetter R.²⁷

Compound Class	Weight % in rye wax	Representative standard	Weight % of standard in rye wax	Weight % of standard in nujol mull
Primary Alcohols	71%	Hexacosanol	69%	72%
Alkyl Esters	11%	Docosyl docosanoate	?	11%
Aldehydes	5%	Octacosanal	0.3%	7%
Alkanes	3%	Hentriacontane and Nonacosane	1.7%	4%
Steroids	0.3%	-	-	-
Alkylresorcinols	3%	AR 25 and AR 19	1%	3%
Others (Secondary Alcohols, Fatty Acids, etc.)	3%	Hexacosanoic Acid	1%	2%
Unknown	2%	-	-	-

The artificial wax mixture was used as a model analyte system to determine if the Raman spectrum seen of extracted rye wax could be reproduced. Consequently, the Raman

spectrum of the artificial wax mixture was directly compared with the Raman spectrum of wax extracted from fresh rye leaves. The overlaid spectra along with the difference between the two are shown in Figure 2.7.

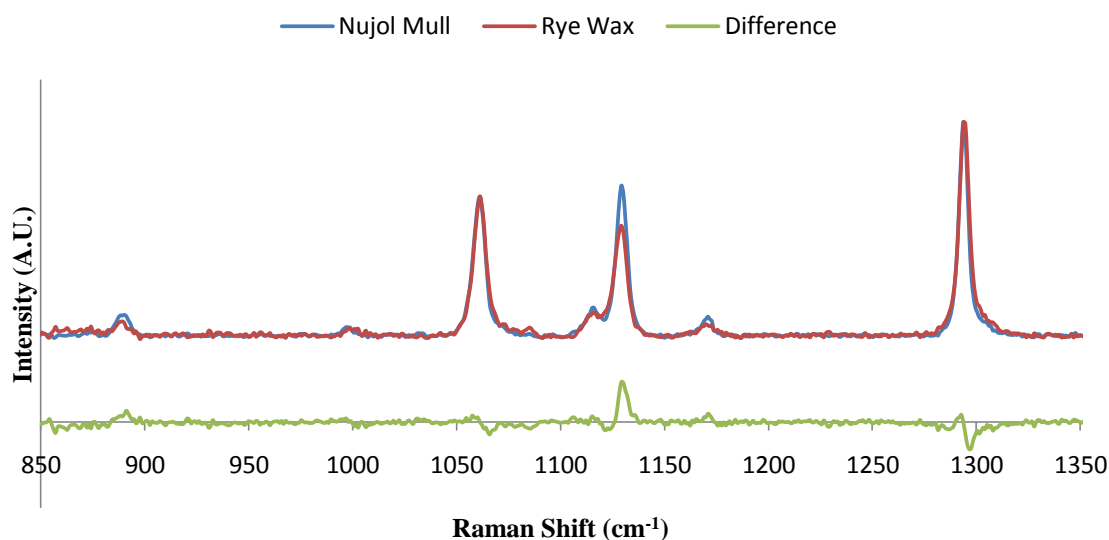


Figure 2.7 Raman spectra of extracted rye wax and the nujol mull (artificial rye wax) along with their difference.

The above spectra show many similarities, however, they do not match exactly. The largest differences are in the amplitudes of the alkyl-related signals and can be attributed to the difference in hydrocarbon chain lengths of the compounds in rye wax from the standards used to represent them. For example in Table 2.1 aldehydes represent 5% of total rye wax. However, the standard available to represent them, $C_{26}H_{52}O$, only represented 0.3% by weight because the most abundant aldehyde, $C_{28}H_{56}O$, was unavailable. The alkyl chain length affects the signal amplitudes for alkylresorcinols as was shown in Figure 2.4, where it can be seen that longer alkyl chains have stronger signals. The hydrocarbon chain length should also affect the signal strength for other compounds in the wax mixture, although perhaps not in exactly the same way. The small differences in some signal amplitudes were not a major concern for the initial analysis because the primary goal was the detection of alkylresorcinols. Furthermore, while the amplitudes did not match exactly, the signal frequencies were the same in both spectra. The signal amplitude differences, however, would cause a problem for quantification that would come later in the development of this method. As can be seen in Figure 2.7 the signal which represents the alkylresorcinol compound class,

1000 cm^{-1} , is quite small in comparison to the noise and other signals. Despite these drawbacks the signal was still detectable in both the rye wax and the artificial rye wax mixture meriting further investigation.

The CMs of rye leaves were isolated and subjected to Raman spectroscopic analysis. The results obtained from the analysis were inconsistent. The marker signal associated with alkylresorcinols compounds was rarely observed and, if a signal at 1000cm^{-1} was observed, it was too weak to quantify. Consequently, the results obtained were inconclusive; they indicated that alkylresorcinols are either present in very specific locations of the CMs, or that their concentrations are below the detection limit attainable with the current instrument. It was also observed that rye CMs contain trichome cells. An attempt was made to acquire spectra from the trichome cells; however, the fact that they protruded from the surface coupled with their thinness resulted in no Raman spectra showing significant signals being obtained. The lack of signals from the alkylresorcinol compounds is likely due to the thinness of the CM and its wax coating. Consequently, the concentrations of alkylresorcinols within the analytical volume are just too small. Despite the lack of alkylresorcinol signals, the Raman spectrum of the CM did show signals representing the aliphatic compounds present in rye wax as well as a few other signals which can be attributed to the CM's cutin matrix. The Raman spectrum of a rye CM is shown below in Figure 2.8.

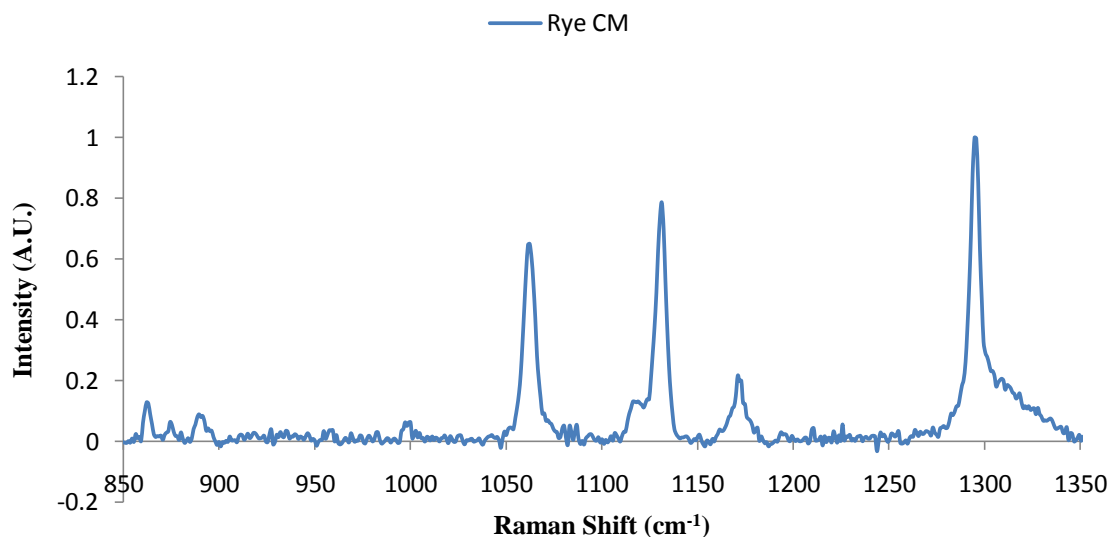


Figure 2.8 Raman spectrum of rye CM.

It should be noted in this chapter that all spectra were acquired without using the confocal capability of the microscope. The Raman spectra of solid standards in confocal mode were obtainable without difficulty; however, when the confocal mode was used to acquire spectra from the rye CMs, the signals were very weak. Since most signals could not be distinguished from the noise, all the spectra had to be acquired with a large slit width and therefore could not be measured in confocal mode. The resulting loss of z-resolution would likely have been problematic when applied to the *in situ* analysis of rye leaves, due to the larger signals originating from background components. However, this stage of analysis was not reached during the work of this thesis and consequently the problem was not addressed. The analysis of the rye CMs was not affected because, while there are two layers of wax, the intracuticular and the epicuticular, the confocal mode of the microscope does not have enough resolving power to distinguish between the two. Although this analysis proved unsuccessful with the current instrumentation, in principle the technique shows great promise as the detection limit of new technology steadily increases. This is due to the fact that the 1000 cm^{-1} marker signal for alkylresorcinols appears to be located in a region of the wax spectrum relatively devoid of peaks from other constituents.

2.4 Conclusion

The analysis of alkylresorcinols in rye cuticles was attempted to obtain lateral distributions over the leaf surface and further the development of Raman microspectroscopy for CM analysis. Initial results showed the presence of a distinct alkylresorcinol signal which was easily differentiated from the other components of the wax. This signal was also present in extracted rye wax and an artificial wax mixture formed using standards, although the signal-to-noise ratio was poor. Attempting the analysis with rye CMs resulted in inconsistent results which could not be analysed. Consequently the investigation involving rye went no further. However, the increasing resolution and detection limits of Raman microscope systems show promise for the analysis of alkylresorcinols in rye cuticles in the future. In the current work no additional plants were investigated for alkylresorcinol content as the rye plant has one of the highest known concentrations of alkylresorcinols among cereal grains. In addition, the general wax composition for other possible candidates was not available.

Chapter 3: Lycopene and Triterpenoids in Tomatoes

The nutritional content of food stocks is important to the overall health of the human population. The ability to determine whether a sample of fruit has a desired nutrient, medicinal compound, or structural component in substantial quantities without destroying the fruit is of great interest to the general public as well as to the food processing industry. Ideally, the analysis should be non-destructive and capable of distinguishing where in the fruit the compound or nutrient is located, for example whether it is on the surface or deep within the tissue. These desirable traits can then be used as criteria to select a suitable method of analysis. This chapter examines the utility of Raman microspectroscopy for mapping the location of triterpenoids and lycopene in tomato skin and more specifically the CM. These compounds are of interests due to their positive health effects as discussed in Chapter 1 as well as in the following section.

3.1 Introduction

The mapping and quantification of triterpenoids has been previously accomplished in the CMs of *Prunus laurocerasus* leaves by Raman microspectroscopy.^{1,21} The analysis of triterpenoids using this technique in other species, however, has not yet been explored. Tomato waxes have been previously analysed, most commonly by GC-MS, for triterpenoids and their bulk concentrations are known.⁸¹⁻⁸⁶ The ease of access to these previously analyzed species prompted their examination as a model fruit for this work. The most abundant triterpenoids found in tomato waxes are α -, β -, and δ -amyrin whose structures are shown in Figure 3.1.^{81,84,85}

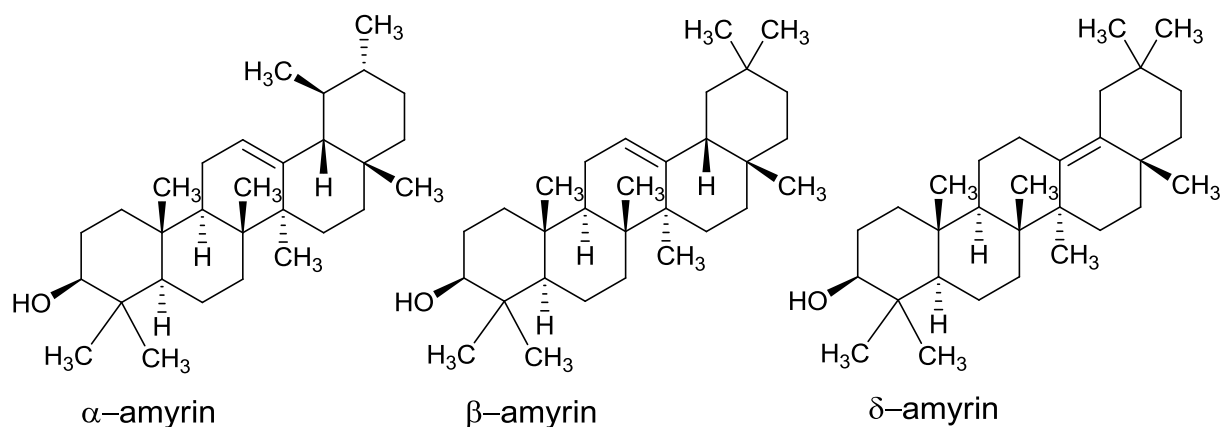


Figure 3.1 Structures of triterpenoids α -, β -, and δ -amyirin.

The previous detection and quantification of triterpenoids in tomato waxes makes them a good candidate to further the study of triterpenoids using Raman microspectroscopy. Even though triterpenoids are not of nutritional interest, per se, as discussed in Chapter 1 they are of interest due to their health effects.

Lycopene, the other analyte investigated in this chapter, is a compound of nutritional value and tomatoes and tomato products are thought to provide the largest source of dietary lycopene.^{45,46} Lycopene, as discussed previously in Chapter 1, is of interest due to its potential positive health effects in the human body. Since tomatoes contain the largest amount of dietary lycopene, they have been the focus of many studies. Tomato-based products including ketchup, tomato paste, tomato sauce, etc. all involve processing of tomatoes and inevitably tomato waste. The concentration of lycopene within some of these products as well as their waste (particularly tomato skin) has been analyzed by HPLC, although results have not all been consistent.^{87,88}

The amount of lycopene in tomatoes varies by cultivar, harvest stage, and storage and processing conditions.⁸⁹⁻⁹¹ Within a tomato fruit, lycopene shows a gradient with increasing concentration moving from the innermost tissues to the exterior.⁹² The largest concentration is found in the epidermal tissue.⁹² Many studies have been done on the tomato skin which, although ill-defined, most commonly includes the cuticle and epidermal cells. Lycopene concentrations have been reported for “whole” tomato skin; however, it has never been reported specifically in the CM.^{93,94}

The present work investigates Raman microspectroscopy as a technique for the investigation of lycopene and triterpenoids in tomato fruit CMs.

3.2 Materials and Methods

3.2.1 Raman spectroscopy system parameters

All spectra were acquired in extended mode from 350 cm^{-1} to 2000 cm^{-1} , except lycopene and the epidermal remnants ($350\text{-}1800\text{ cm}^{-1}$). The laser power was set to 100% for all spectra except hentriacontane (50%) and all spectra were acquired with a 50x (0.75 NA) objective. The image area on the CCD was set to have a three pixel width thus increasing the resolution in the x-y plane and the binning was set to two. The detector time was set to between 10-100 seconds. All tomato CM measurements were integrated for 60 s, except the green CM which was 20 s; hentriacontane, lycopene, and wax were 10 s; epidermal remnants were 30 s, while α - and β -amyrin were 100 s. 1-20 accumulations were acquired (lycopene, α - and β -amyrin (1), red CM (3), yellow CM (5), green CM (9), hentriacontane (2), epidermal remnants (4), and wax (20)). The slit width was set to $100\text{ }\mu\text{m}$ for all samples except for lycopene and the epidermal remnants where it was set to $10\text{ }\mu\text{m}$.

3.2.2 Reference materials

α - and β -amyrin were obtained from Fluka (Switzerland). Lycopene and hentriacontane was obtained from Sigma-Aldrich (Oakville, Ontario, Canada). All compounds were used as received. The spectra were collected at different points on the same solid sample and compared to ensure that there were no significant differences in the spectra of the same standard reflecting inhomogeneities from the preparation.

3.2.3 Wax extraction

Tomato plants were grown under ambient conditions in the Jetter lab at The University of British Columbia and the fruit were harvested for analysis. Approximately 80% of the tomato fruit surface area was dipped for $\sim 30\text{ s}$ in a beaker containing approximately 30 mL of pure chloroform (Fisher Scientific, Ontario) to avoid extraction from the point of

attachment (the tomato stem).⁸¹ The tomato was then transferred to a second beaker and the process was repeated to ensure all wax had been extracted. The chloroform extracts were then combined into one beaker and left in a fume hood to evaporate.

3.2.4 Digestion of cell walls

Tomatoes were cut to remove the skin which was then used to isolate the CM by Orgell's technique as modified by Yamada et al., Petracek and Bukovac.⁷²⁻⁷⁴ The skin pieces were then placed in a 20 mL scintillation vial containing 2% (w/w) cellulase (INC Biomedicals, Aurora, Ohio), 2% (w/w) pectinase (Fluka, Switzerland), and 1 mM sodium azide (NaN₃) in 5 mL citrate buffer. The pieces were left to digest for 3 days. After digestion was complete the isolated CMs were placed in NanopureTM water in a Petri dish and floated over a hole pierced into a piece of aluminum foil and left to dry. Later in analysis CMs were sonicated before they were floated on the aluminum foil to remove epidermal remnants.

3.3 Results and Discussion

The selection of an appropriate sample is always an important first step in any analysis. For example, in the previous chapter a selection was made between rye leaves or grains, and in this chapter, the question is which ripeness stage of the tomato to examine in terms of its amenability to Raman microspectroscopy for CM analysis. It has been previously shown that the concentration of triterpenoids at different ripeness stages, excluding immature green fruit which was not examined here, are similar.⁸⁵ It was initially thought that flavonoids and carotenoids, the compounds mostly responsible for the tomato's color, might interfere with the Raman analysis of triterpenoids in the tomato CMs. Consequently, tomato CMs were isolated at different stages of ripeness (mature green, yellow, and red). It was noted that, after isolation, epidermal remnants remained on the internal side of the CM (the side which was in contact with the cells).⁸² Raman analyses continued without removal of these remnants since the interest was in the exterior side, which contained the waxes. The normalized Raman spectra of the green, yellow, and red CMs are shown in Figure 3.2.

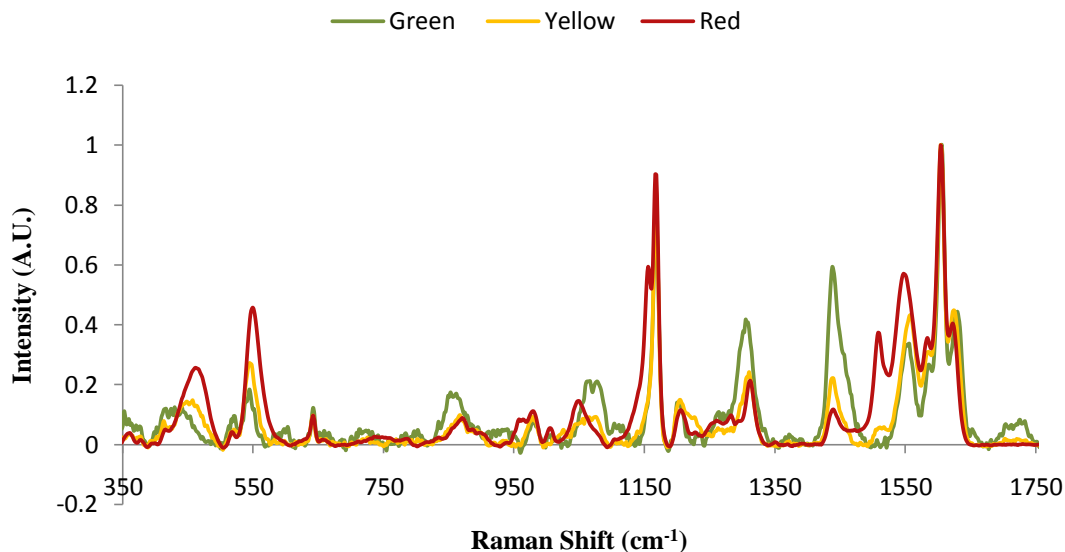


Figure 3.2 Normalized Raman spectra of tomato fruit CMs. The color is the color of the tomato skin and all spectra are normalized to the tallest signal.

The spectra shown above are very similar, as most of the signals overlap. The signals associated with triterpenoids should appear predominantly in the lower wavenumber region of the spectrum ($350\text{-}800\text{ cm}^{-1}$). It has been previously shown that in this region the triterpenoid signals should not overlap with the aliphatic signals, making them distinguishable.¹ The large similarities between spectra of the different-coloured tomato CMs in Figure 3.2 indicate that the pigment compounds do not produce interfering signals and are, consequently, not an issue in the current analysis of tomato waxes. At higher wavenumbers there are a few signals which do not overlap and they will be discussed later. Consequently, red tomatoes were used for further analysis of triterpenoids and lycopene as they provided the most intense Raman signals in the shortest acquisition time.

As mentioned earlier, α -, β -, and δ -amyrin are the most abundant triterpenoids in tomatoes. Unlike with the alkylresorcinols in rye leaves it has already been established that triterpenoids are distinguishable from the aliphatic wax components in Raman spectra. However, the exact signal frequencies for the triterpenoids of interest still need to be established. Consequently, standards of α - and β -amyrin were used to collect reference spectra; however, δ -amyrin was unavailable. The Raman spectra are shown below in Figure 3.3 along with the spectrum of the red tomato CM.

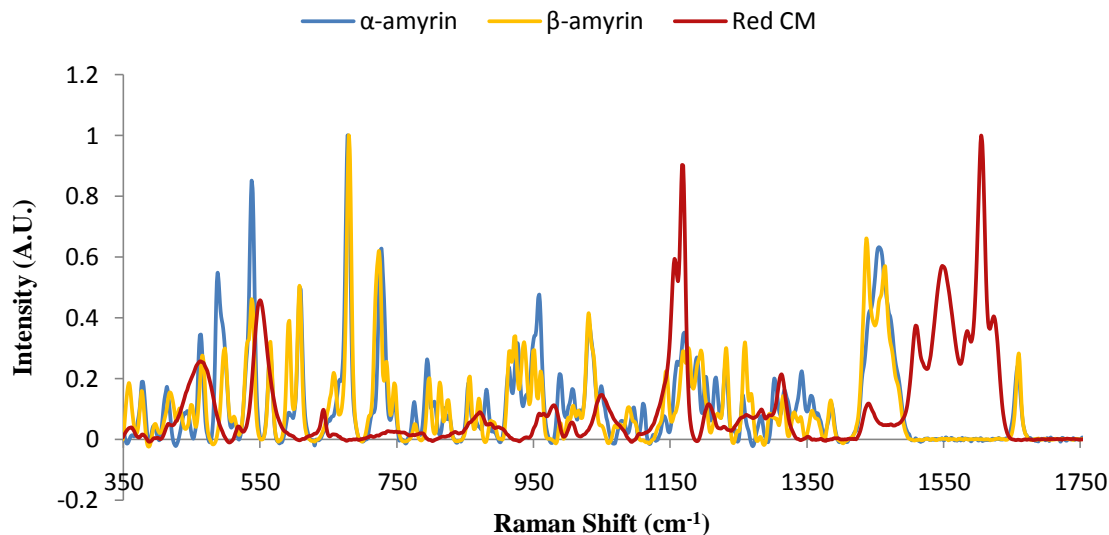


Figure 3.3 Normalized Raman spectra of α - and β -amyrin along with red tomato fruit CM. All spectra are normalized to the tallest signal.

The figure above shows that α - and β -amyrin have many overlapping signals. The red tomato CM, however, does not contain readily distinguishable α - and β -amyrin signals. The lack of triterpenoid signals in the CM spectrum could arise from either inadequate instrument detection limit or the masking of signals by another component of the CM. In order to further investigate the origin of the problem, the wax and the cutin matrix needed to be examined separately. Consequently, wax was extracted from red tomatoes, and a Raman spectrum of both the extracted wax alone and the cutin matrix alone was obtained. The Raman spectrum of the wax along with that of the most abundant aliphatic compound found in tomato wax, hentriacontane ($C_{31}H_{64}$ saturated alkane), is shown below in Figure 3.4.

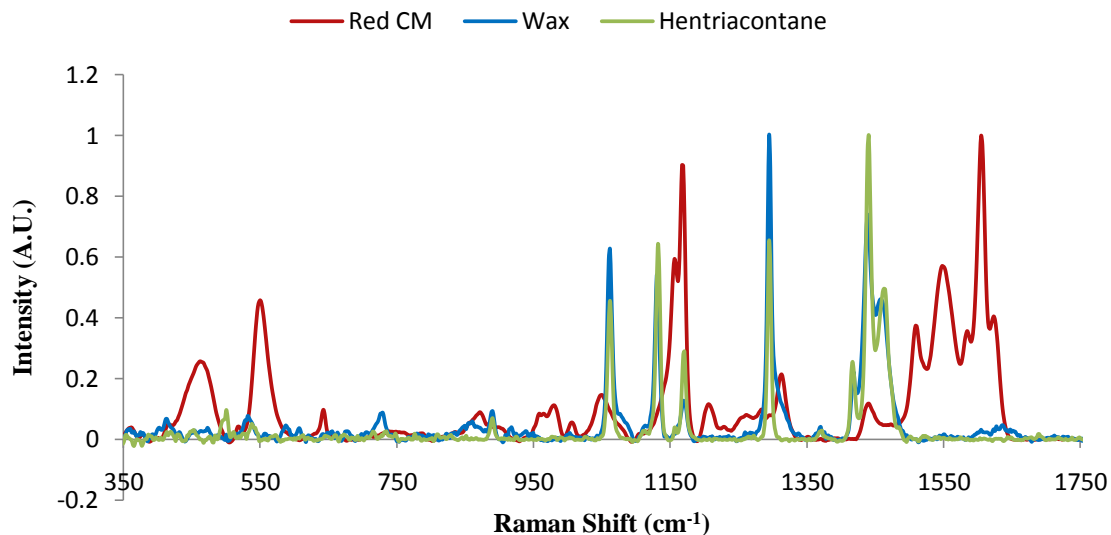


Figure 3.4 Normalized Raman spectra of a tomato fruit CM, tomato fruit wax, and hentriacontane. All spectra are normalized to the tallest signal.

As expected, the above spectra show that the hentriacontane and the tomato wax share many of the same signals. The wax does show a signal at 727 cm^{-1} which could be representative of α - and β -amyrin. Thus, the wax does show signs of what could be a signal from triterpenoids although they could not be detected in the intact CM. The wax, however, does not show many of the other signals observed in the intact tomato CM, indicating that the signals from the tomato CM originate from the cutin matrix. A Raman spectrum of the cutin matrix (CM with wax removed), the tomato fruit CM, and their difference is shown in Figure 3.5.

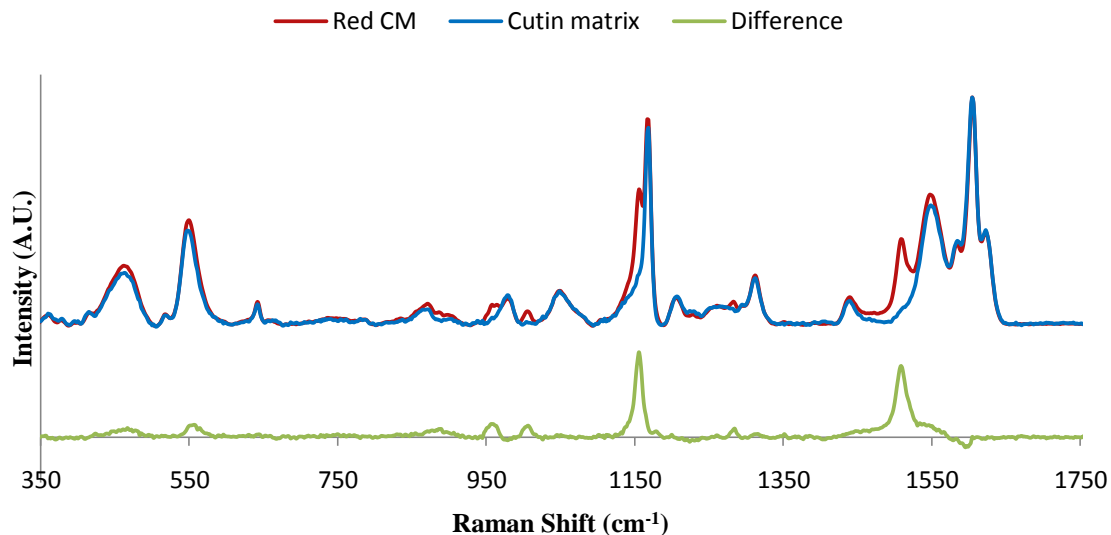


Figure 3.5 Raman spectra of red tomato fruit CM, cutin matrix and their difference.

It can be seen in the above figure that most of the signals are accounted for by the cutin matrix. In fact many of the major signals from the cutin matrix are similar to those reported for a polysaccharide fraction isolated from tomato CMs.⁹⁵ These polysaccharides should theoretically have been removed during digestion. However, unlike some CMs from other species, tomato's CMs extend through multiple cell layers. Consequently the CM becomes more intertwined with cells, which can make it more difficult to digest all of the polysaccharides. The length of the digestion was changed to see if any more pectin or cellulose could be removed and the results showed no significant differences. However, this is not unexpected as it has been reported previously that tomato CMs after digestion still contain cellulose.⁹⁶ The Raman spectrum of undigested tomato skin was also taken and resulted in virtually the same spectrum being observed, even though there was a visual difference in the appearance of the subepidermal tissue between digested and undigested tomato skin. It thus became apparent that no definitive triterpenoid signals could be observed in the Raman spectrum of tomato CMs. This is most likely due to the masking effect of the intense polysaccharide signals and this is not an obstacle that can be overcome with the current method of digestion. The cutin matrix and some polysaccharides become integrated during CM development and tomato CMs extend over many layers of cells as mentioned previously.^{13,95,96} The combination of these facts makes it difficult to obtain a Raman

spectrum without any interference from polysaccharides. An attempt was made to use the confocal modality of the microscope to limit the amount of signal collected from the cutin but the results showed no signs of triterpenoids and the polysaccharide signals remained. Consequently, the mapping of triterpenoids in the tomato fruit was not possible with the current method. However, the difference between the tomato CM and the cutin matrix (Figure 3.5) shows that there are still Raman signals that are unaccounted for.

These unidentified signals match the Raman spectrum of lycopene previously reported from tomato puree.⁴⁶ It is important to note that lycopene is responsible for the red color of tomatoes and consequently these signals should not be observed in either the green or yellow tomato CMs. This can be seen in Figure 3.2 as only the red CM spectrum shows lycopene signals although the yellow CM spectrum shows a small signal which is consistent with β -carotene.⁴⁶ The Raman spectrum of pure lycopene was obtained and the results are shown below in Figure 3.6 overlaid on top of the difference spectrum (representing the soluble portion of the tomato fruit CM) from Figure 3.5.

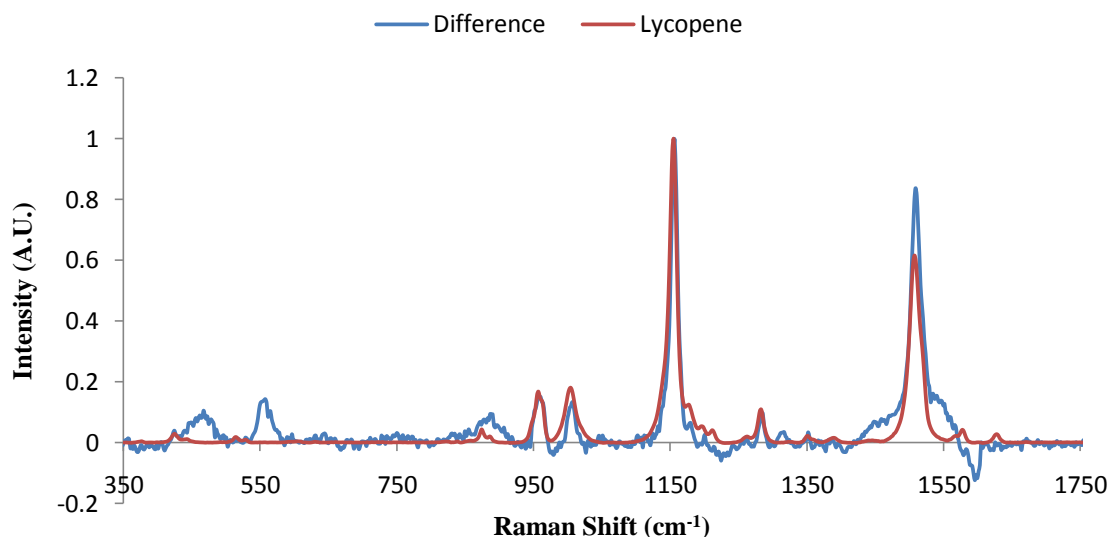


Figure 3.6 Normalized Raman spectra of the difference (tomato fruit CM – CM without wax) and lycopene.

The presence of lycopene in tomatoes is well documented as described in the introduction (section 3.1). While it has been found in the epidermal tissue of the tomato fruit, it has not yet been reported in the CM of the tomato. This prompted a re-examination of the procedure

to assess whether or not this observation was novel and significant, or an artefact of the preparation.

When the CMs were originally isolated, the epidermal remnants were not removed, as mentioned previously. The CMs had a reddish color; however, no pigment compounds have been reported in tomato CMs before. This color suggests the possible presence of lycopene and, consequently, the epidermal remnants that had originally not been removed from the tomato CM were re-examined separately. The remnants were removed from the CM using a paint brush followed by sonication of the sample. A Raman spectrum of the epidermal remnants is shown below along with the spectrum of pure lycopene in Figure 3.7.

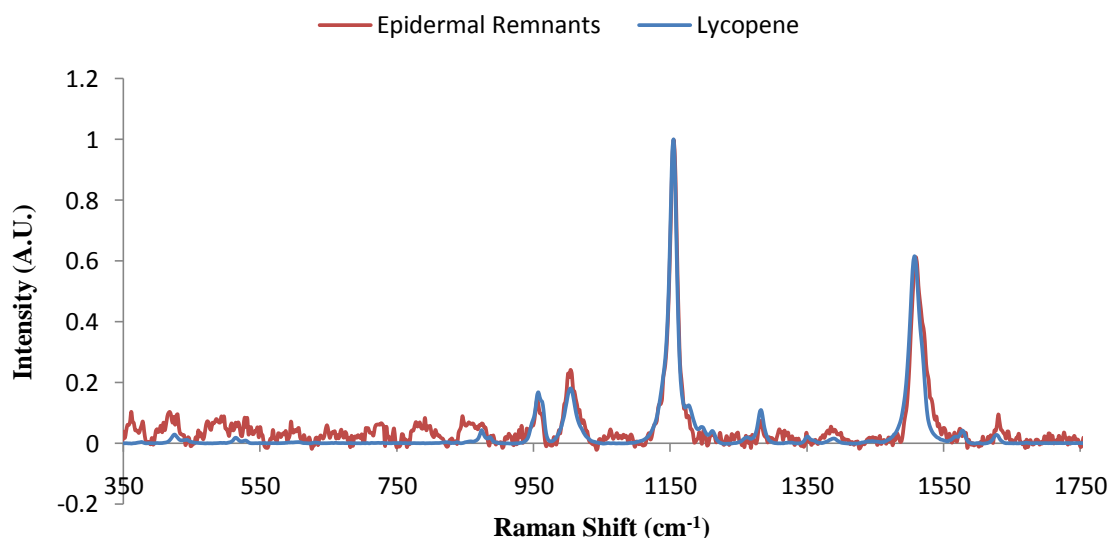


Figure 3.7 Normalized Raman spectra of tomato fruit CM epidermal remnants (remnants of cells after digestion of cell walls) and lycopene.

The above spectra show that the epidermal remnants did in fact contain lycopene. After removal of the epidermal remnants the Raman spectrum of the tomato CM was retaken. The resulting spectrum showed the absence of signals associated with lycopene and the spectrum (data not shown) looked like that in Figure 3.2 for the green and yellow tomatoes, showing only the signals associated with the cutin matrix and polysaccharides. Thus, it was concluded that there is no detectable lycopene in tomato CMs and that the epidermal remnants were responsible for the lycopene features evident in the difference spectrum of Figure 3.5.

3.4 Conclusion

The analysis of triterpenoids and lycopene in tomato CMs using Raman microspectroscopy was attempted. The results showed no measureable sign of any triterpenoid signals in the CM, but there was a representative signal in the Raman spectrum of concentrated red tomato wax. The CM spectra showed large signals attributed to polysaccharides, indicating a potential problem with the method of digestion. However, since the cutin matrix and some polysaccharides can become integrated, the polysaccharides avoid complete removal by simple enzymatic digestion; a straightforward modification of the adopted protocol would not likely yield significant improvement. A suitable solution would require the development of a new or substantially modified protocol which was beyond the intended scope of this investigation. If a protocol that successfully extracts the interfering polysaccharide components from the CM becomes available, then it may be worth re-examining the utility of Raman microspectroscopy for studies of triterpenoids in the tomato CM.

Analysis of the red tomato CM data using difference spectroscopy resulted in the unexpected detection of lycopene. However, it was subsequently shown that the epidermal remnants contained all of the detectable lycopene and therefore it was not present in the CM itself. This is consistent with other findings since no lycopene has yet been reported in the CM of tomatoes.

Chapter 4: Application of Raman Microspectroscopy to the Analysis of Triterpenoids in Cuticular Membranes

The application of Raman microspectroscopy to the analysis of plant, including fruit, cuticles is attempted in this chapter. Many different samples were analysed providing information about possible applications of this technique in the future. In general, however, the technique did not yield sufficiently useful results to merit further exploration for quantitative analyses at this time. This chapter first presents CMs on which triterpenoid analysis was attempted along with the information gained from each sample. The results are then combined to provide guidelines which could be used to aid those attempting analysis of triterpenoids by Raman microspectroscopy in CMs in the future.

4.1 Introduction

Plants, including fruit, have been the focus of many studies for their potential nutritional, agricultural, and medicinal value, in addition to their fundamental scientific value. Many plant CMs have been previously studied using a variety of analytical techniques including *Kalanchoe daigremontiana*, *Ligustrum vulgare*, *Rosa canina* (rose) leaf, bell peppers and *Prunus avium* (cherry fruit) to name a few.⁹⁷⁻¹⁰³ However, these previous studies in general have not been successful in revealing detailed spatial distributions of many analytes of interest, such as triterpenoids. Such “chemical imaging” applications in other fields have often been successfully addressed using Raman microspectroscopy. Therefore, analysis of *Kalanchoe daigremontiana*, *Ligustrum vulgare*, *Rosa canina*, bell peppers and *Prunus avium* (cherry fruit) samples (along with others) using Raman microspectroscopy was attempted. The combined knowledge gained from these analyses and the data presented in previous chapters is considered here in an effort to define the limits to quantification or detection of triterpenoids in CMs. A brief introduction will be given for each species examined where relevant.

4.2 Materials and Methods

4.2.1 Raman spectroscopy system parameters

All spectra were acquired with a 50x (0.75 NA) objective. The spectra were acquired in extended mode from 350-1800 cm^{-1} for all samples except the *Kalanchoe daigremontiana* and *Ligustrum vulgare* CMs which were from 350-2000 cm^{-1} . The laser power was set to 100% (35-45 mW) except for the *Ligustrum vulgare* CM where the power was 25%. The image area on the CCD was set to have a three pixel width thus increasing the resolution in the x-y plane and the binning was set to two. The detector time was set to 60 seconds for all samples. The accumulations were between 5-40 (10 for all samples except rose CM (20), rose cutin matrix (40), and all cherry samples (100)). The slit width was set to 100 μm for all samples except the rose where the slit was set to 10 μm .

The data for section 4.2.4 was acquired on the upgraded (inVia) Raman system; all other data was acquired using the original (RM 1000) system. The parameters for the data in section 4.2.4 are as follows: Photobleaching was accomplished by leaving the samples under the laser at 100% power for a recorded period of time (30 minutes for spectrum in Figure 4.9). The spectrum was acquired in extended mode from 350-1800 cm^{-1}) with a slit width of 50 μm and a laser power of 100%. The detector time was 10 seconds and there was only one accumulation.

4.2.2 Reference materials

Glutinol was isolated by Clare Van Maarseveen in the Jetter lab at The University of British Columbia.¹⁰⁰ Nonacosane, hentriacontane, and ursolic acid were obtained from Sigma-Aldrich (Oakville, Ontario, Canada). All compounds were used as received. The spectra were collected at different points on the same solid sample and compared to ensure that there were no significant differences in the spectra of the same standard.

4.2.3 Plant and fruit samples

Bing cherries (*Prunus avium*) used for analysis were purchased at a local farmers market. Rose (*Rosa canina*) leaves were obtained from a long stem rose purchased at a local

florist. *Ligustrum vulgare* leaves were obtained from plants grown continuously in a garden in central Europe (Munich, Germany). The *Kalanchoe daigremontiana* plants were grown under ambient conditions in the Jetter lab at The University of British Columbia. The leaves were harvested when they were large enough that the cuticle could be isolated, but the precise age of the plants was unknown. *Prunus laurocerasus* fruit were grown outdoors under ambient conditions in Vancouver, BC and the fruit was harvested when mature.

4.2.4 Digestion of cell walls

Cherries (both *Prunus avium* and *Prunus laurocerasus*) were cut with razor blade to remove the skin; *Ligustrum vulgare* and *Rosa canina* leaf pieces were cut out of a leaf using scissors; and *Kalanchoe daigremontiana* skin was pulled off using tweezers. These pieces were then used to isolate the CMs by Orgell's technique as modified by Yamada et al. and Petracek and Bukovac.⁷²⁻⁷⁴ The pieces were then placed in a 20 mL scintillation vial containing 2% (w/w) cellulase (INC Biomedicals, Aurora, Ohio), 2% (w/w) pectinase (Fluka, Switzerland), and 1 mM sodium azide (NaN_3) in 5 mL citrate buffer. The pieces were left to digest for a different number of days depending on the sample: cherry (*Prunus avium*) six days, *Kalanchoe daigremontiana* two days, *Prunus laurocerasus* 10 days, *Rosa canina* and *Ligustrum vulgare* 13 days). The digest was changed every 2-4 days so ensure complete digestion. After digestion was complete the isolated CMs were placed in Nanopure™ water and sonicated. Then placed in a Petri dish and floated over a hole pierced into a piece of aluminum foil and left to dry.

4.2.5 Wax extraction, and GC analysis

The wax was extracted from *Prunus laurocerasus* fruit by submerging the fruit in ~30 mL of chloroform for two minutes. The chloroform was then evaporated to dryness and a small amount (<1mL) of chloroform was used to dissolve the wax from the beaker and transfer it into a vial. The wax was then analyzed according to the guidelines outlined in the following reference, but no internal standard was used.¹⁰⁴

4.3 Results

The analysis of several different model samples was carried out to the best of the capabilities of the available technology and the results are summarized below. In each case the results of the analyses are briefly discussed in terms of why quantification was not successful. The results are then discussed in terms of the knowledge gained which could be applied to future attempts at cuticular analyses by Raman microspectroscopy. It was learned that, in many cases, information that can be obtained from the literature before the study is attempted, could provide a good indication as to whether or not the Raman analysis would be successful. This chapter specifically focuses on CMs of *Prunus avium* (cherry) fruit, *Kalanchoe daigremontiana*, *Ligustrum vulgare*, *Rosa canina* (rose), and *Prunus laurocerasus* fruit.

4.3.1 Cherry fruit (*Prunus avium*)

The cherry fruit skin is of interest due to fruit cracking, which is a problem among many cultivars as it destroys the fruit as well as making it unappealing to customers. The reason for this skin cracking is not completely understood. The results of studies to date have found a relationship between fruit cracking and the structure of the epidermis, surface characteristics relating to water and gas transport, and cuticle thickness.^{105,106} The composition of the fruit CM could also play a role. The cherry fruit cuticular waxes, which make up part of the CM, have been shown to have a very high concentration of triterpenoids.¹⁰³ Since the composition of the CM is of interest, the distribution of triterpenoids across the cherry cuticle using Raman microspectroscopy was attempted.

The Raman spectra of cherry wax along with nonacosane and ursolic acid are shown in Figure 4.1. Nonacosane and ursolic acid are used to represent the most abundant aliphatic and triterpenoid compounds, respectively, found in cherry wax and their structures are shown in Figure 4.2.¹⁰³

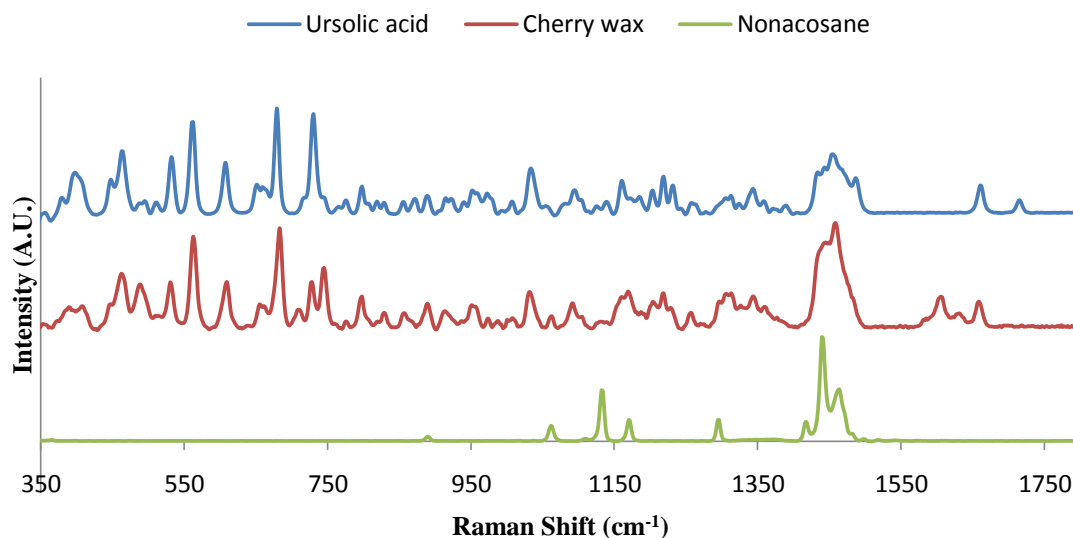


Figure 4.1 Raman spectra of cherry fruit wax, nonacosane, and ursolic acid.

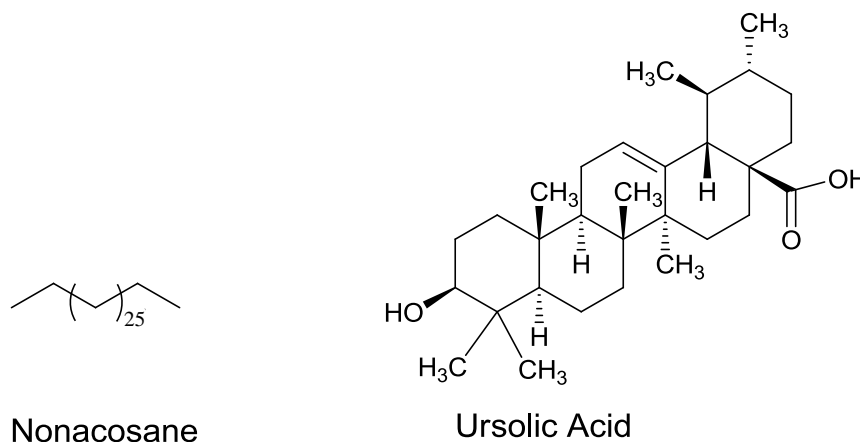


Figure 4.2 Structures of nonacosane and ursolic acid.

The spectra show many overlapping signals for ursolic acid and cherry wax, though not for nonacosane and cherry wax. The presence of significant triterpenoid signals in the cherry wax spectrum prompted further analysis. The Raman spectra of the cherry CM and the cutin matrix (CM without wax) were collected and are shown together with their difference spectrum and the cherry wax spectrum in Figure 4.3.

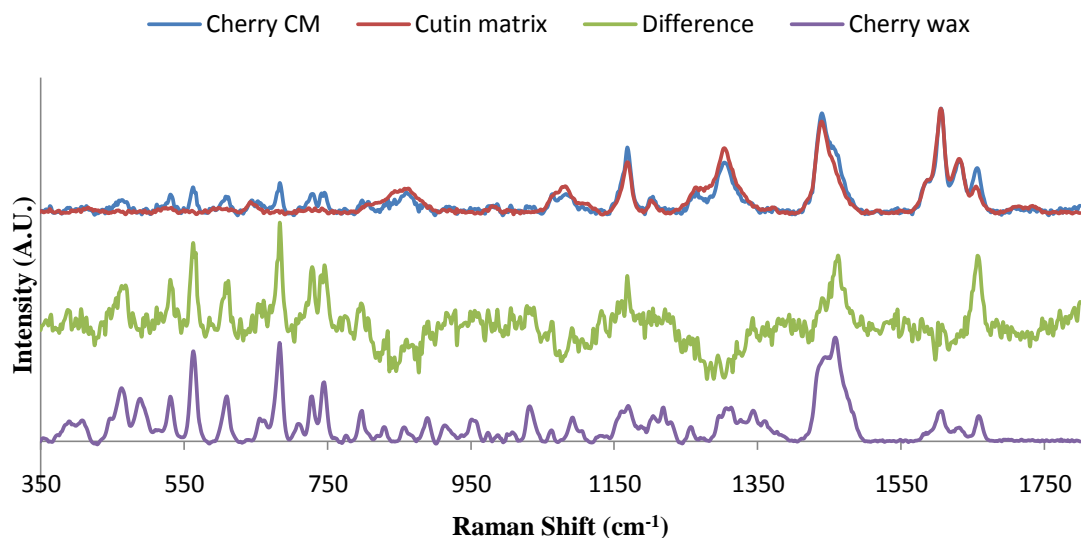


Figure 4.3 Raman spectra of a cherry fruit CM, cutin matrix, and the difference between the two; also shown is a spectrum of cherry fruit wax for comparison.

The difference spectrum shows many signals in the lower wavenumber region previously associated with triterpenoids. These signals are also found in the cherry wax spectrum, which is expected as the cherry wax and the difference spectra should be the same (CM - cutin matrix = wax). The difference spectrum was then compared to the spectra for nonacosane and ursolic acid. The results are shown in Figure 4.4.

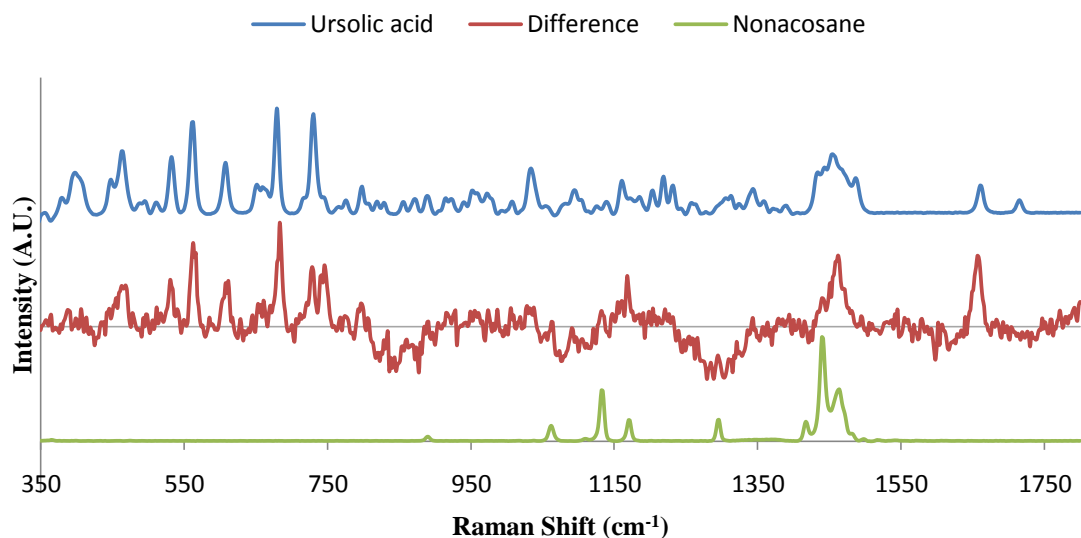


Figure 4.4 Raman spectra of ursolic acid, and nonacosane, together with the difference spectrum from Figure 4.3. The gray line on the difference spectrum shows the zero-difference axis.

The ursolic acid signals overlap with many of the signals in the difference spectrum unlike the nonacosane signals. Specifically the nonacosane signal at approximately 1132 cm⁻¹ cannot be resolved in the difference spectrum. The result is that, while the triterpenoid signals are well above the baseline, they cannot be compared to the aliphatics which are the other main wax component. Without this component signal for comparison, the relative quantification of triterpenoids cannot be completed. However, with an improvement in the sensitivity of Raman microspectroscopy or the application of a more sensitive technique the quantification of triterpenoids in cherry wax is a very realistic possibility.

4.3.2 *Kalanchoe daigremontiana*

The composition of *Kalanchoe daigremontiana* leaf waxes has recently been investigated in detail using GC.^{100,101} They have been shown to contain the relatively uncommon triterpenoids glutinol and friedelin whose structures are shown in Figure 4.5.¹⁰⁷⁻

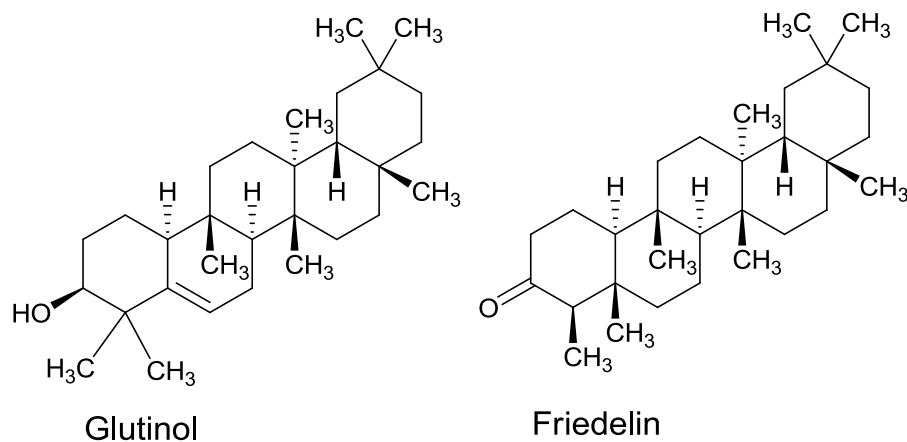


Figure 4.5 Structures of glutinol and friedelin.

The investigation of the CM of the *Kalanchoe daigremontiana* leaves using Raman microspectroscopy was undertaken to explore the potential of this technique for quantification of these compounds. *Kalanchoe daigremontiana* plants of the same age as those previously studied were initially unavailable and consequently initial analysis was completed on much older plants while others were being grown. Raman spectra of the *Kalanchoe daigremontiana* leaf CM along with its most abundant aliphatic and triterpenoid components, reported for the younger specimens, were obtained and the results are shown in Figure 4.6.

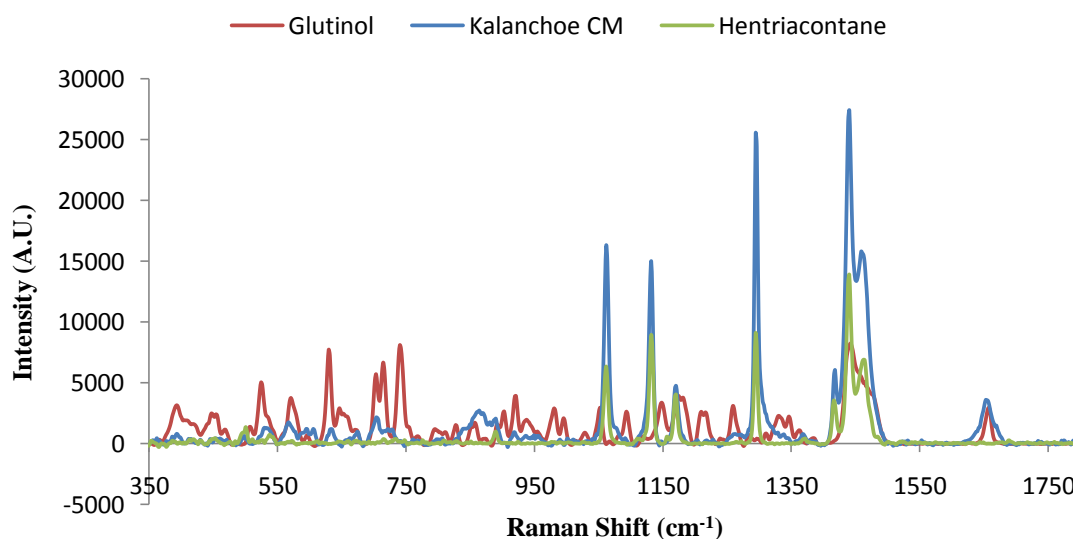


Figure 4.6 Raman spectra of glutinol, *Kalanchoe daigremontiana* leaf CM, and hentriacontane.

The *Kalanchoe daigremontiana* leaf CM spectrum and the hentriacontane spectrum contain many overlapping signals. Therefore, Figure 4.6 shows that the *Kalanchoe daigremontiana* leaf CM contains alkane signals as expected based on its previously reported composition. The spectrum also contains triterpenoid signals, as shown by the overlapping signals in the 350-800 cm^{-1} region. Although the signals are quite weak, in comparison to the alkane ones, there is some potential for triterpenoid analysis and consequently more plants were grown. It was discovered that, when the *Kalanchoe daigremontiana* plants had reached the age corresponding to the specimens examined in previous studies, the leaf CM was too thin to mechanically isolate. Consequently, no further analysis was completed, however the appearance of both aliphatic and triterpenoid signals in the spectra merit further investigation. There are a couple of possible options for the direction this research could take: The development of a new isolation method for the CMs of younger *Kalanchoe daigremontiana* leaves, or a time course to determine when the CM becomes isolatable by the current method and the analysis of the waxes at that stage followed my Raman microspectroscopic analysis.

4.3.3 *Ligustrum vulgare* and *Rosa canina* leaves

Ligustrum vulgare and *Rosa canina* (rose) leaves have been previously analyzed for triterpenoids in their cuticular waxes by GC.^{97,99,104} *Ligustrum vulgare* leaf waxes have a relatively high concentration of triterpenoids, especially when compared to *Rosa canina* leaf waxes, suggesting that Raman analysis may be suitable for investigating their spatial distribution. *Rosa canina* leaves were analyzed due to their availability and the accessibility of literature data, however, it should be noted that the literature data is for a different variety of *Rosa canina* than the one analyzed. The results turned out to have related obstacles which will be discussed later.

The Raman spectra of a *Ligustrum vulgare* CM and the cutin matrix are shown below in Figure 4.7.

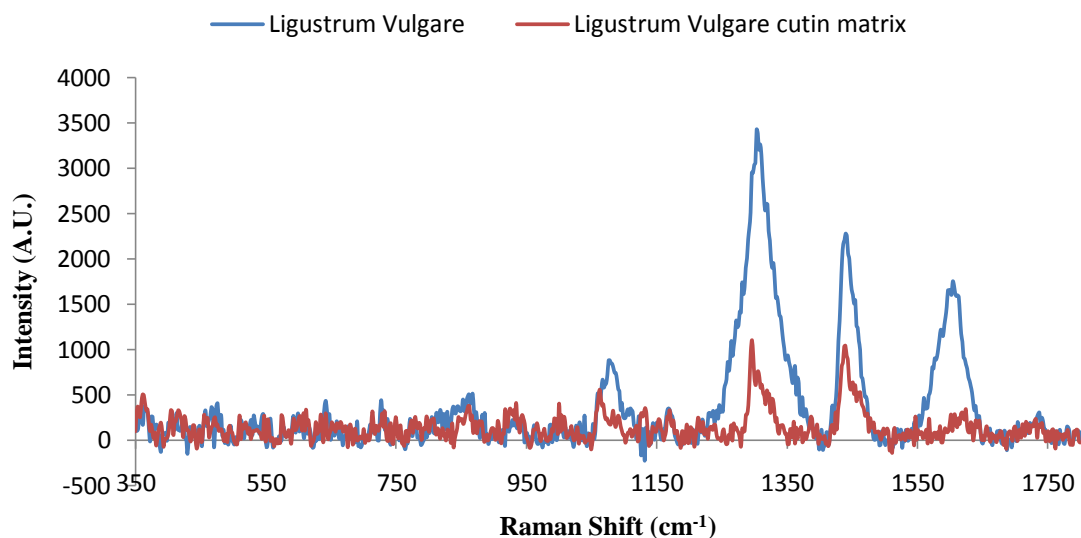


Figure 4.7 Raman spectra of *Ligustrum vulgare* leaf CM and its cutin matrix.

The spectra show that the only distinguishable signals originate from the cutin matrix and not from the wax. This is similar to the results obtained for the *Rosa canina* CM, as shown in Figure 4.8, where no triterpenoid signals are resolvable in the lower wavenumber region. In these cases the cutin matrix could in theory be analyzed. However, this matrix has been previously well characterized as discussed in Chapter 1. Furthermore, the composition of the cutin matrix is not known to have large variability between species and consequently the Raman spectra should not differ greatly, thus, limiting the ability of Raman to provide any novel information.

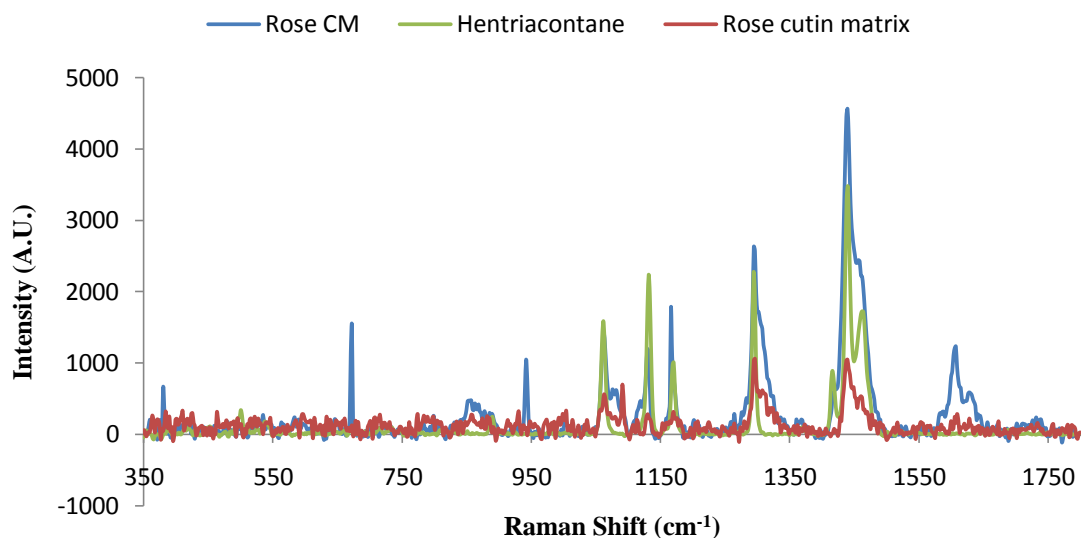


Figure 4.8 Raman spectra *Rosa canina* (rose) leaf CM, hentriacontane, and the rose cutin matrix.

In the case of the *Ligustrum vulgare* and the *Rosa canina* (rose) leaf there are no triterpenoid signals visible in the spectra of the CM. Consequently, quantification cannot be achieved in these species using Raman microspectroscopy. However, there are some aliphatic signals in the *Rosa canina* spectrum as shown by the signals overlapping between the rose CM and hentriacontane spectra in Figure 4.8. Consequently, the rose CM may be amenable to Raman analysis in the future as sensitivity increases or with a more sensitive technique.

4.3.4 *Prunus laurocerasus* fruit

The leaf CMs of *Prunus laurocerasus* have previously been successfully analyzed for triterpenoids as mentioned earlier.¹ However, there is no literature on the fruit wax or CMs of *Prunus laurocerasus*. Consequently, a GC analysis of the *Prunus laurocerasus* fruit wax was completed to confirm that, like the *Prunus laurocerasus* leaf, the most abundant triterpenoid found in the wax is ursolic acid. The result showed this to be true with the fruit wax containing ~27% ursolic acid. An attempt was then made to detect triterpenoids in the mature fruit CMs; however, the background in the spectra was initially so high that it saturated the detector masking any usable signals. The sample was photobleached by leaving it under the

laser (100% power) before analysis. This was somewhat successful as some signals became visible after photobleaching as seen in Figure 4.9 along with the spectrum of ursolic acid.

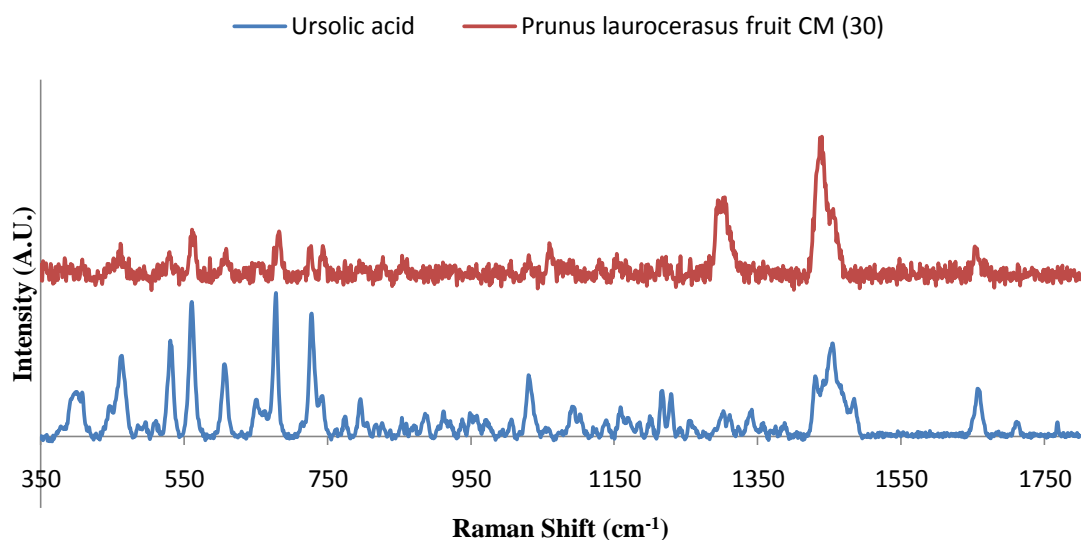


Figure 4.9 Raman spectra of ursolic acid and *Prunus laurocerasus* fruit CM. The 30 represents the photobleaching time in minutes.

The signal at 561 cm⁻¹ appears in both spectra in Figure 4.9 although the signal at 678 cm⁻¹ in the ursolic acid spectrum does not align well with the signal at 682 cm⁻¹ in the *Prunus laurocerasus* fruit CM spectrum. However, the complete composition of the fruit wax is not currently known and there is a signal which corresponds to ursolic acid as well as other signals in the region previously associated with triterpenoids. Consequently, further work in this area is required to fully analyze the *Prunus laurocerasus* fruit wax and CM. There does appear to be significant potential for analysis using Raman microspectroscopy once data from other chemical methods becomes available for comparison.

4.4 Discussion

The species examined in this chapter as well as in Chapter 3 each provide reasons why Raman microspectroscopic analysis could not be applied for quantification of triterpenoids in the CM of some plant species. In the case of *Kalanchoe daigremontiana* the reason is the simple inability to isolate the CM due to its lack of strength and thickness. The

ability to isolate the cuticle plays a key role in being able to analyse it and improved protocols for doing so are needed in order to exploit Raman microspectroscopy for studying triterpenoid distributions. In the case of *Prunus laurocerasus* fruit there were initial problems with background luminescence, which could be addressed using *in situ* photobleaching, but the unavailability of data on CM wax composition prevented meaningful comparative analysis. These are potentially addressable reasons why the analysis could not be carried out on other species. However, the reasons why Raman microspectroscopy had limited value for analyzing the cuticle of some other samples whose wax composition is known and whose CM can be isolated merit further discussion.

Based on knowledge gained during these exploratory investigations it appears that there are a few specific factors that play a role in whether or not a sample can be analyzed, beyond the inability to isolate the cuticle or the lack of sufficient supporting information. These factors include the amount of triterpenoids within the wax, the amount of wax within the CM (which consists mostly of cutin), and the wax coverage of the cuticle. These data can be found in the literature or determined from previously published data, even if not explicitly calculated in the reported results. The results of a literature search for those samples analyzed are summarized in Table 4.1.

Table 4.1 The approximate percentage of triterpenoids within the wax, wax within the CM, and wax coverage in some analyzed species. Along with a summary of the guidelines derived. *Prunus laurocerasus* is shown for comparison with previous work.

Name	Percentage of Triterpenoids in the Wax	Percentage of Wax in the CM	Wax Coverage ($\mu\text{g}/\text{cm}^2$)
<i>Rosa canina</i> leaf CM	~14% ⁹⁷	unknown	~28 ⁹⁷
<i>Ligustrum vulgare</i> leaf CM	~66% ¹⁰⁴	~12% ¹¹⁰	~27 ¹⁰⁴ - 40 ¹¹⁰
Cherry (<i>Prunus avium</i>) fruit CM	~76% ¹⁰³	~18% ¹⁰³	~20 ¹⁰³
<i>Prunus laurocerasus</i> leaf CM	~11% ⁶²	~25% ¹¹⁰	~45 ⁶² - 83 ¹¹⁰
Tomato fruit CM	~10% ⁸¹	unknown	~15 ⁸¹
Summary	10-60%	>20%	>30

The results in the table above show some informative trends when compared to the data previously analyzed. The rose leaf cuticle (*Rosa canina*) has a relatively small percentage of triterpenoids which may account for the lack of triterpenoid signals in the rose leaf CM Raman spectrum (Figure 4.8), however, it should be noted that the variety of *Rosa canina* analyzed and the one shown in the table above were not the same. Literature data was unavailable for the analyzed rose leaf; therefore, the entry in the table above is listed as an approximate value. The *Ligustrum vulgare* on the other hand has a relatively high percentage of triterpenoids to wax, but a relatively low percentage of wax in the CM. Based only on the relative percentage of triterpenoids, one might expect that they should be detectable, however, due to the low relative percentage of wax, the concentrations of both triterpenoids and aliphatics are likely below the detection limit of the Raman microscope (Figure 4.7). This difference is accentuated by the wax coverage where *Ligustrum vulgare* has approximately half the amount of wax ($\mu\text{g}/\text{cm}^2$) when compared with the *Prunus laurocerasus* which has been previously successfully analyzed.¹ While *Prunus laurocerasus* has a relatively low percentage of triterpenoids in the wax, it has a high percentage of wax in the CM and a large wax coverage, allowing for detection and quantification. The cherry fruit has a very high percentage of triterpenoids; therefore, the signals attributed to those

compounds are very strong (Figure 4.1 and 4.4). However, there is not a high enough concentration of aliphatic compounds to detect and therefore, the triterpenoids cannot be quantified. The tomato CM discussed in Chapter 3 is also shown in the table and it should be noted that considering it is relatively small wax coverage it is doubtful that triterpenoid signals could be detected even if a better digestion method was developed.

The last row of Table 4.1 summarizes the approximate ranges of the discussed parameters which could lead to a successful Raman analysis of triterpenoids in a CM. Consequently, when looking at CMs for triterpenoids it is important to assess the viability of a given specimen using the parameters displayed in Table 4.1 if available. Another large obstacle to consider with Raman analysis of any CM is the thickness, in all cases discussed above the isolated CM was <10 μm thick which is less than the confocal resolution of the Raman microscope. However, even with this limitation the analysis has proven to have great potential. It should be noted that Raman analysis was also attempted on bell peppers, *Macaranga tanarius* stem, and castor bean stem CM. In the case of the *Macaranga tanarius* and castor bean stems CMs there were no signals detectable above the background, while for the bell pepper the cutin matrix signals masked the other signals much like the *Ligustrum vulgare* and the rose leaf. Consequently, these results are not discussed as they provided no new insight into the difficulties of Raman microspectroscopic analysis.

This discussion has focussed specifically on triterpenoids. Bringing this together with the alkylresorcinol data from Chapter 2, a couple points can be made. Since only one species, rye, was analyzed for alkylresorcinols no general guidelines can be drawn. However, considering that alkylresorcinols account for only 3% by weight of the rye leaf wax and that the wax coverage is $\sim 12 \mu\text{g}/\text{cm}^2$ combined with the fact that the alkylresorcinols were detectable in wax and occasionally in the CM, it is clear that the limits of alkylresorcinol detection would be much lower than those for triterpenoids.²⁷

4.5 Conclusion

The CMs of a variety of species were examined for triterpenoids. A selection of them was shown here to demonstrate the insights gained by their analysis. There are a variety of

reasons why CM analysis for triterpenoids may not be feasible in certain species. The main points are inability to isolate the cuticle, availability of general wax composition data, the percentage of triterpenoids in the wax, the percentage of wax in the CM, and the wax coverage. The quantitative analysis of triterpenoids in the cuticle was not successful for any of the species attempted, but it allowed for exploration of the limitations of Raman microspectroscopy for this type of analysis. The increasing detection limits available on future instruments may allow for the analysis of triterpenoids in some of the CMs attempted in this work.

Chapter 5: Conclusions and Future Work

The goal of this research was to survey plant CMs to assess the applicability of Raman microspectroscopy for quantitative analysis. While quantification of compounds in the CMs analyzed was not successful, knowledge was gained about the obstacles facing this type of analysis. This is particularly true for the triterpenoids, which are one of the most interesting classes of analytes. The work described in previous chapters outlines the procedures for preparation and analysis of plant CMs, as well as the potential challenges involved.

5.1 Concluding Remarks

The utility for analysis of alkylresorcinols and triterpenoids in plant materials using Raman microspectroscopy was explored in this work. The results of the alkylresorcinol examinations presented in Chapter 2 demonstrated that, while these compounds can be detected in rye leaf wax, they can rarely be detected in the rye leaf CM. The lack of a consistent alkylresorcinol signal resulted in the inability to complete quantitative analysis. The high concentration of alkylresorcinols in rye compared with other possible plant species resulted in a move away from alkylresorcinol analysis.^{24,69} However, the fact that the aliphatic signals were present and the alkylresorcinols signals were occasionally observed merits further investigation as the sensitivity of instruments increases. Since triterpenoids had previously been analyzed in *Prunus laurocerasus* CMs, the possible extension of this analysis to other species was explored.¹

The attempt at tomato analysis was presented in Chapter 3, but the large signal from the polysaccharides of the tomato CM made triterpenoids undetectable. However, Raman analysis of the CM resulted in the detection and identification of lycopene which, if not an artefact, was an interesting observation as it has never previously been reported in tomato CM. Upon re-examination of the experimental procedure it was found that the CM contained epidermal remnants after being digested which were red in color. The removal of these

remnants by brushing and sonication resulted in the disappearance of the lycopene signals. Consequently, considering the lack of triterpenoid signals, no further analyses involving tomato CMs were carried out. The application of more intensive digestions techniques to tomato CMs could allow for them to be re-examined with Raman microspectroscopy for triterpenoids, however, since tomato's have a relatively small wax coverage, noted in Chapter 4, it is doubtful that triterpenoids would be detectable.

In Chapter 4, a series of other species were examined for the presence of triterpenoids. These samples were chosen for their known bulk triterpenoid concentration, literature data, and sample availability. The results of these experiments were largely unsuccessful, in terms of quantifying triterpenoid distributions, but qualitative observations were combined with those from previous experiments to reach conclusions about the general applicability of Raman microspectroscopy for triterpenoid analysis in plant CMs. Various factors were examined which can aid in determining whether or not Raman analysis of a particular plant species (with sufficient supporting data available from the literature) would likely be successful. These factors include: the ability to isolate the intact cuticle, the relative amount of triterpenoids in the wax, the relative amount of wax in the CM (weight percent), and the wax coverage. Some of this data can be found in the literature and can be used to assess whether or not a proposed analysis has sufficient potential to warrant proceeding. This simple pre-assessment could potentially save many hours of trial and error experimentation and, as such, is an important outcome of this project.

In the case of the specific species investigated here, Raman analysis for quantification was not successful. However, future analysis of triterpenoids in some of these plant CMs using Raman microspectroscopy may become feasible if, for example, the detection limit of the instrumentation, specifically the signal-to-noise ratio, significantly increases. The exploration of new compounds and new species by Raman microspectroscopy is still a viable option, however care must be taken to ensure that selected samples have high enough concentrations of the compounds of interest relative to the wax component to make the analyses attempts worthwhile.

5.2 Future Work

The work outlined in this thesis has provided a number of guidelines for the analysis of triterpenoids in plant CMs. These guidelines are potentially applicable to other plant species. While none of the current analyses were successful, with technological innovations, different species, and different compounds Raman analysis has a high potential for success.

The detection limit of the instrument and the signal-to-noise ratio are two of the difficulties which need to be overcome for the analyses of this work to be successful. Newer technology could bring with it lower detection limits, better signal-to-noise ratios, and faster analysis times. Furthermore, there are other Raman techniques which could be applied particularly those which provide signal enhancement such as tip enhanced Raman spectroscopy. While the mechanism of action of this enhancement is not completely understood, as understanding increases, the ability for this technique to supply quantitative information is a possibility. Consequently, some of the analyses which were not successful here may be viable in the future. However, even if the analyses are not viable there are also other species and compound classes which have yet to be explored. The advantage of Raman spectroscopy to provide *in situ* information without destruction of the sample is desirable, but the means by which to attain this goal are not as simple as point and shoot. The development of a reliable method resulting in a successful Raman analysis of CMs has the potential to provide a wealth of information which is currently unavailable.

The guidelines outlined in Chapter 4 specifically in Table 4.1 gave possible directions for future research. A literature search resulted in two possible candidates that fall within those proposed guidelines: the *Humulus lupulus* (hop) leaf and the *Castanea sativa* (sweet chestnut) leaf. The *Humulus lupulus* leaf has 22% triterpenoids within its wax and 62 $\mu\text{g}/\text{cm}^2$ wax coverage and the *Castanea sativa* leaf has 32% triterpenoids within its wax and 48 $\mu\text{g}/\text{cm}^2$ wax coverage.^{111,112} In both cases there is a significant percentage of triterpenoids in the wax but more importantly there is a large wax coverage which should allow for detection and quantification of triterpenoids. The final criteria, percent wax in the CM could not be found for these species; however, it is the most difficult of the guidelines to find in the literature. Despite lacking data for this guideline, both species have a high probability of being successful for Raman microspectroscopic analysis.

This work used isolated plant CMs, but the ideal case is to move from an isolated CM to the intact leaf or fruit from which the CM was isolated. This will provide more challenges, as the background Raman scattering from cell components will complicate analyses; however, the ultimate goal is to use Raman spectroscopy non-destructively on intact specimens thus eliminating complicated and time consuming sample preparation.

REFERENCES

- (1) Yu, M. M. L., University of British Columbia, 2008.
- (2) Raman, C. V.; Krishnan, K. S. *Nature* **1928**, *121*, 501-502.
- (3) Petry, R.; Schmitt, M.; Popp, J. *ChemPhysChem* **2003**, *4*, 14-30.
- (4) Ferraro, J. R.; Nakamoto, K.; Brown, C. W. *Introductory Raman Spectroscopy*; 2 ed.; Academic Press: Boston, 2003.
- (5) *Handbook of Raman Spectroscopy: from the research laboratory to the process line*; Lewis, I. R.; Edwards, H. G. M., Eds.; Marcel Dekker: New York, 2001.
- (6) Hirschfeld, T. *Journal of the Optical Society of America* **1973**, *63*, 476-477.
- (7) Puppels, G. J.; Otto, C.; Greve, J. *Trac-Trends Anal. Chem.* **1991**, *10*, 249-253.
- (8) Minsky, M. *Scanning* **1988**, *10*, 128-138.
- (9) Tabaksblat, R.; Meier, R. J.; Kip, B. J. *Appl. Spectrosc.* **1992**, *46*, 60-68.
- (10) Gallardo, A.; Spells, S.; Navarro, R.; Reinecke, H. *J. Raman Spectrosc.* **2007**, *38*, 880-884.
- (11) Reina-Pinto, J. J.; Yephremov, A.; Elsevier France-Editions Scientifiques Medicales Elsevier: Bordeaux, FRANCE, 2008, p 540-549.
- (12) Riederer, M. In *Biology of the Plant Cuticle*; Riederer, M., Muller, C., Eds.; Blackwell Publishing: Iowa, 2006; Vol. 23, p 1-8.
- (13) Jeffree, C. E. In *Biology of the Plant Cuticle*; Riederer, M., Muller, C., Eds.; Blackwell Publishing: Iowa, 2006; Vol. 23, p 11-125.
- (14) Purves, W. K.; Orians, G. H.; Heller, H. C. *Life: The Science of Biology*; 4 ed.; W.H. Freeman & Co.: Salt Lake City, 1995.
- (15) Jetter, R.; Kunst, L.; Samuels, A. L. In *Biology of the Plant Cuticle*; Riederer, M., Muller, C., Eds.; Blackwell Publishing: Iowa, 2006; Vol. 23, p 145-181.
- (16) Kolattukudy, P. E. *Can. J. Bot.-Rev. Can. Bot.* **1984**, *62*, 2918-2933.
- (17) Heredia, A. *Biochim. Biophys. Acta-Gen. Subj.* **2003**, *1620*, 1-7.
- (18) Nip, M.; Tegelaar, E. W.; Deleeuw, J. W.; Schenck, P. A.; Holloway, P. J. *Naturwissenschaften* **1986**, *73*, 579-585.
- (19) Nip, M.; Deleeuw, J. W.; Holloway, P. J.; Jensen, J. P. T.; Sprenkels, J. C. M.; Depooter, M.; Sleenckx, J. J. M. *J. Anal. Appl. Pyrolysis* **1987**, *11*, 287-295.
- (20) Holloway, P. J. In *The Plant Cuticle*; Cutler, D. F., Alvin, K. L., Price, C. E., Eds.; Academic Press: London, 1982, p 1-32.
- (21) Yu, M. M. L.; Konorov, S. O.; Schulze, H. G.; Blades, M. W.; Turner, R. F. B.; Jetter, R. *Planta* **2008**, *227*, 823-834.
- (22) Knodler, M.; Berardini, N.; Kammerer, D. R.; Carle, R.; Schieber, A. *Rapid Commun. Mass Spectrom.* **2007**, *21*, 945-951.
- (23) Droby, S.; Prusky, D.; Jacoby, B.; Goldman, A. *Physiol. Mol. Plant Pathol.* **1987**, *30*, 285-292.
- (24) Ross, A. B.; Shepherd, M. J.; Schupphaus, M.; Sinclair, V.; Alfaro, B.; Kamal-Eldin, A.; Aman, P. *J. Agric. Food Chem.* **2003**, *51*, 4111-4118.

- (25) Diogenes, M. J. N.; deMoraes, S. M.; Carvalho, F. F. *Contact Dermatitis* **1996**, *35*, 114-115.
- (26) Kozubek, A.; Tyman, J. H. P. *Chem. Rev.* **1999**, *99*, 1-25.
- (27) Ji, X.; Jetter, R. *Phytochemistry* **2008**, *69*, 1197-1207.
- (28) Reffstrup, T.; Hammershoy, O.; Boll, P. M.; Schmidt, H. *Acta Chemica Scandinavica Series B-Organic Chemistry and Biochemistry* **1982**, *36*, 291-294.
- (29) Garcia, S.; Garcia, C.; Heinzen, H.; Moyna, P. *Phytochemistry* **1997**, *44*, 415-418.
- (30) Ross, A. B.; Kamal-Eldin, A.; Aman, P. *Nutr. Rev.* **2004**, *62*, 81-95.
- (31) Korycinska, M.; Czelna, K.; Jaromin, A.; Kozubek, A. *Food Chemistry* **2009**, *116*, 1013-1018.
- (32) Liu, J.; Liu, Y. P.; Parkinson, A.; Klaassen, C. D. *J. Pharmacol. Exp. Ther.* **1995**, *275*, 768-774.
- (33) Liu, J. *J. Ethnopharmacol.* **1995**, *49*, 57-68.
- (34) Liu, J. *J. Ethnopharmacol.* **2005**, *100*, 92-94.
- (35) Li, J.; Guo, W. J.; Yang, Q. Y. *World J. Gastroenterol.* **2002**, *8*, 493-495.
- (36) Oliveira, F. A.; Lima, R. C. P.; Cordeiro, W. M.; Vieira, G. M.; Chaves, M. H.; Almeida, F. R. C.; Silva, R. M.; Santos, F. A.; Rao, V. S. N. *Pharmacol. Biochem. Behav.* **2004**, *78*, 719-725.
- (37) Sunitha, S.; Nagaraj, M.; Varalakshmi, P. *Fitoterapia* **2001**, *72*, 516-523.
- (38) Katerere, D. R.; Gray, A. I.; Nash, R. J.; Waigh, R. D. *Phytochemistry* **2003**, *63*, 81-88.
- (39) Yun, B. S.; Ryoo, I. J.; Lee, I. K.; Park, K. H.; Choung, D. H.; Han, K. H.; Yoo, I. D. *J. Nat. Prod.* **1999**, *62*, 764-766.
- (40) Mahato, S. B.; Sarkar, S. K.; Poddar, G. *Phytochemistry* **1988**, *27*, 3037-3067.
- (41) Bohm, V.; Puspitasari-Nienaber, N. L.; Ferruzzi, M. G.; Schwartz, S. J. *J. Agric. Food Chem.* **2002**, *50*, 221-226.
- (42) Mortensen, A.; Skibsted, L. H. *J. Agric. Food Chem.* **1997**, *45*, 2970-2977.
- (43) Stahl, W.; Sies, H. *Arch. Biochem. Biophys.* **1996**, *336*, 1-9.
- (44) Mangels, A. R.; Holden, J. M.; Beecher, G. R.; Forman, M. R.; Lanza, E. *J. Am. Diet. Assoc.* **1993**, *93*, 284-296.
- (45) Omoni, A. O.; Aluko, R. E. *Trends in Food Science & Technology* **2005**, *16*, 344-350.
- (46) Baranska, M.; Schutz, W.; Schulz, H. *Anal. Chem.* **2006**, *78*, 8456-8461.
- (47) Baranski, R.; Baranska, M.; Schulz, H. *Planta* **2005**, *222*, 448-457.
- (48) Brandt, S.; Pek, Z.; Barna, E.; Lugasi, A.; Helyes, L. *J. Sci. Food Agric.* **2006**, *86*, 568-572.
- (49) Clei • ment, A.; Dorais, M.; Vernon, M. *J. Agric. Food Chem.* **2008**, *56*, 9813-9818.
- (50) Ollanketo, M.; Hartonen, K.; Riekkola, M. L.; Holm, Y.; Hiltunen, R. *Eur. Food Res. Technol.* **2001**, *212*, 561-565.
- (51) Rao, A. V.; Waseem, Z.; Agarwal, S. *Food Res. Int.* **1998**, *31*, 737-741.
- (52) Canet, D.; Rohr, R.; Chamel, A.; Guillain, F. *New Phytol.* **1996**, *134*, 571-577.
- (53) Ray, A. K.; Chen, Z. J.; Stark, R. E. *Phytochemistry* **1998**, *49*, 65-70.

- (54) Kolattukudy, P. E. *Science* **1980**, *208*, 990-1000.
- (55) Fang, X. H.; Qiu, F.; Yan, B.; Wang, H.; Mort, A. J.; Stark, R. E.; Pergamon-Elsevier Science Ltd: San Francisco, California, 2000, p 1035-1042.
- (56) Zlotnikmazori, T.; Stark, R. E. *Macromolecules* **1988**, *21*, 2412-2417.
- (57) Szafranek, B.; Tomaszewski, D.; Pokrzywinska, K.; Golebiowski, M. *Acta Biol. Crac. Ser. Bot.* **2008**, *50*, 49-54.
- (58) Reynhardt, E. C.; Riederer, M. *J. Phys. D-Appl. Phys.* **1991**, *24*, 478-486.
- (59) Orban, N.; Kozak, I. O.; Dravucz, M.; Kiss, A. *Int. J. Food Sci. Technol.* **2009**, *44*, 869-873.
- (60) Koch, K.; Ensikat, H. J. *Micron* **2008**, *39*, 759-772.
- (61) Kerstiens, G. *J. Exp. Bot.* **1996**, *47*, 1813-1832.
- (62) Jetter, R.; Schaffer, S.; Riederer, M. *Plant Cell Environ.* **2000**, *23*, 619-628.
- (63) Gierlinger, N.; Schwanninger, M. *Spectr.-Int. J.* **2007**, *21*, 69-89.
- (64) Baranska, M.; Baranski, R.; Schulz, H.; Nothnagel, T. *Planta* **2006**, *224*, 1028-1037.
- (65) Schulz, H.; Baranska, M.; Baranski, R. *Biopolymers* **2005**, *77*, 212-221.
- (66) Baranska, M.; Schulz, H.; Joubert, E.; Manley, M. *Anal. Chem.* **2006**, *78*, 7716-7721.
- (67) Schulz, H.; Baranska, M. *Vib. Spectrosc.* **2007**, *43*, 13-25.
- (68) Baranska, M.; Schulz, H.; Siuda, R.; Strehle, M. A.; Rosch, P.; Popp, J.; Joubert, E.; Manley, M. *Biopolymers* **2005**, *77*, 1-8.
- (69) Hengtrakul, P.; Mathias, M.; Lorenz, K. *J. Nutr. Biochem.* **1991**, *2*, 20-24.
- (70) Renishaw Spectroscopy Products Division UK, 2000.
- (71) Schulze, G.; Jirasek, A.; Yu, M. M. L.; Lim, A.; Turner, R. F. B.; Blades, M. W. *Appl. Spectrosc.* **2005**, *59*, 545-574.
- (72) Orgell, W. H. *Plant Physiol.* **1955**, *30*, 78-80.
- (73) Petracek, P. D.; Bukovac, M. J. *Plant Physiol.* **1995**, *109*, 675-679.
- (74) Yamada, Y.; Bukovac, M. J.; Wittwer, S. H. *Plant Physiol.* **1964**, *39*, 28-32.
- (75) Tripathi, G. N. R. *J. Chem. Phys.* **1981**, *74*, 250-255.
- (76) Orendorff, C. J.; Ducey, M. W.; Pemberton, J. E. *J. Phys. Chem. A* **2002**, *106*, 6991-6998.
- (77) Lin-Vien, D.; Colthup, N. B.; Fateley, W. G.; Grasselli, J. G. *The Handbook of Infrared and Raman Characteristic Frequencies of Organic Molecules*; Academic Press: Boston, 1991.
- (78) Snyder, R. G.; Schachtschneider, J. H. *Spectrochimica Acta* **1963**, *19*, 85-116.
- (79) Bryant, M. A.; Pemberton, J. E. *J. Am. Chem. Soc.* **1991**, *113*, 8284-8293.
- (80) Thompson, W. R.; Pemberton, J. E. *Anal. Chem.* **1994**, *66*, 3362-3370.
- (81) Vogg, G.; Fischer, S.; Leide, J.; Emmanuel, E.; Jetter, R.; Levy, A. A.; Riederer, M. *J. Exp. Bot.* **2004**, *55*, 1401-1410.
- (82) Hovav, R.; Chehanovsky, N.; Moy, M.; Jetter, R.; Schaffer, A. A. *Plant J.* **2007**, *52*, 627-639.
- (83) Bauer, S.; Schulte, E.; Thier, H. P. *Eur. Food Res. Technol.* **2004**, *219*, 223-228.
- (84) Bauer, S.; Schulte, E.; Thier, H. P. *Eur. Food Res. Technol.* **2004**, *219*, 487-491.

- (85) Mintz-Oron, S.; Mandel, T.; Rogachev, I.; Feldberg, L.; Lotan, O.; Yativ, M.; Wang, Z.; Jetter, R.; Venger, I.; Adato, A.; Aharoni, A. *Plant Physiol.* **2008**, *147*, 823-851.
- (86) Leide, J.; Hildebrandt, U.; Reussing, K.; Riederer, M.; Vogg, G. *Plant Physiol.* **2007**, *144*, 1667-1679.
- (87) Seybold, C.; Frohlich, K.; Bitsch, R.; Tto, K.; Bohm, V. *J. Agric. Food Chem.* **2004**, *52*, 7005-7010.
- (88) Tonucci, L. H.; Holden, J. M.; Beecher, G. R.; Khachik, F.; Davis, C. S.; Mulokozi, G. *J. Agric. Food Chem.* **1995**, *43*, 579-586.
- (89) Raffo, A.; Leonardi, C.; Fogliano, V.; Ambrosino, P.; Salucci, M.; Gennaro, L.; Bugianesi, R.; Giuffrida, F.; Quaglia, G. *J. Agric. Food Chem.* **2002**, *50*, 6550-6556.
- (90) Abushita, A. A.; Daood, H. G.; Biacs, P. A. *J. Agric. Food Chem.* **2000**, *48*, 2075-2081.
- (91) Giovanelli, G.; Lavelli, V.; Peri, C.; Nobili, S. *J. Sci. Food Agric.* **1999**, *79*, 1583-1588.
- (92) Moco, S.; Capanoglu, E.; Tikunov, Y.; Bino, R. J.; Boyacioglu, D.; Hall, R. D.; Vervoort, J.; De Vos, R. C. H. *J. Exp. Bot.* **2007**, *58*, 4131-4146.
- (93) Topal, U.; Sasaki, M.; Goto, M.; Hayakawa, K. *J. Agric. Food Chem.* **2006**, *54*, 5604-5610.
- (94) del Castillo, M. L. R.; Gomez-Prieto, M. S.; Herraiz, M.; Santa-Maria, G. *J. Am. Oil Chem. Soc.* **2003**, *80*, 271-274.
- (95) Lopez-Casado, G.; Matas, A. J.; Dominguez, E.; Cuartero, J.; Heredia, A. *J. Exp. Bot.* **2007**, *58*, 3875-3883.
- (96) Matas, A. J.; Cobb, E. D.; Bartsch, J. A.; Paolillo, D. J.; Niklas, K. J. *Am. J. Bot.* **2004**, *91*, 352-360.
- (97) Buschhaus, C.; Herz, H.; Jetter, R. *Ann. Bot.* **2007**, *100*, 1557-1564.
- (98) Bauer, S.; Schulte, E.; Thier, H. P. *Eur. Food Res. Technol.* **2005**, *220*, 5-10.
- (99) Jenks, M. A.; Andersen, L.; Teusink, R. S.; Williams, M. H. *Physiol. Plant.* **2001**, *112*, 62-70.
- (100) van Maarseveen, C.; Han, H.; Jetter, R. *Plant Cell Environ.* **2009**, *32*, 73-81.
- (101) van Maarseveen, C.; Jetter, R. *Phytochemistry* **2009**, *70*, 899-906.
- (102) Olszewska, M. *Acta Chromatogr.* **2008**, *20*, 643-659.
- (103) Peschel, S.; Franke, R.; Schreiber, L.; Knoche, M. *Phytochemistry* **2007**, *68*, 1017-1025.
- (104) Buschhaus, C.; Herz, H.; Jetter, R. *New Phytol.* **2007**, *176*, 311-316.
- (105) Demirsoy, L.; Demirsoy, H. *Pak. J. Bot.* **2004**, *36*, 725-731.
- (106) Peschel, S.; Beyer, M.; Knoche, M. *Sci. Hortic.* **2003**, *97*, 265-278.
- (107) Gaiand, K. N.; Singla, A. K.; Boar, R. B.; Copey, D. B. *Phytochemistry* **1976**, *15*, 1999-2000.
- (108) Gaiand, K. N.; Gupta, R. L. *Phytochemistry* **1972**, *11*, 1500-&.
- (109) Siems, K.; Jas, G.; Arriagaginer, E. J.; Wollenweber, E.; Dorr, M. *Z.Naturforsch.(C)* **1995**, *50*, 451-454.
- (110) Schreiber, L.; Riederer, M. *Oecologia* **1996**, *107*, 426-432.
- (111) Gulz, P. G.; Muller, E.; Herrmann, T. *Z.Naturforsch.(C)* **1992**, *47*, 661-666.

- (112) Gulz, P. G.; Muller, E.; Herrmann, T.; Losel, P. *Z.Naturforsch.(C)* **1993**, *48*, 689-696.